N O T I C E

THIS DOCUMENT HAS BEEN REPRODUCED FROM
MICROFICHE. ALTHOUGH IT IS RECOGNIZED THAT
CERTAIN PORTIONS ARE ILLEGIBLE, IT IS BEING RELEASED
IN THE INTEREST OF MAKING AVAILABLE AS MUCH
INFORMATION AS POSSIBLE

FINAL TECHNICAL REPORT

SYNTHESIS OF REGIONAL CRUST AND UPPER-MANTLE STRUCTURE
FROM SEISMIC AND GRAVITY DATA

Submitted to

National Aeronautics and Space Administration

Grant No: NSG 5276
15 June 1978 - 14 June 1979

by

S S. Alexander
Principal Investigator
403 Deike Building
814-865-2622

P. M. Lavin
Co-Investigator
443 Deike Building
814-865-3951

Department of Geosciences
The Pennsylvania State University
University Park, Pennsylvania 16802

SNYTHESIS OF REGIONAL CRUST AND UPPER-MANTLE STRUCTURE

FROM SEISMIC AND GRAVITY DATA

Abstract

The principal objective of this study is to combine available seismic and ground-based gravity data to infer the three-dimensional crust and upper mantle structure in selected regions. This snythesis and interpretation proceeds from large-scale average models suitable for early comparison with high-altitude satellite potential field data to more detailed delineation of structural boundaries and other variations that may be significant in natural resource assessment. While the study focuses primarily on seismic and ground based gravity data, other relevant information (e.g. magnetic field, heat flow, Landsat imagery, geodetic leveling, natural resources maps) are used to constrain the structure inferred and to assist in defining structural domains and boundaries. The relevant seismic data base consists of regional refraction lines, limited reflection coverage, surface wave dispersion, teleseismic P and S-wave delay times, anelastic absorption (Q), and regional seismicity patterns. The gravity data base consists of available point gravity determinations for the areas considered. The primary area considered is the Eastern United States from the Mississippi River to the Atlantic Continental Margin.

The interpretation makes use of modern inversion methods, digital analysis techniques, and empirical evidence on density-seismic velocity relationships for crustal rocks. Results of the first year's study under NASA Grant No. NSG 5276 are summarized in this report.

SUMMARY

The first year of this investigation (under Grant NSG 5276) has been devoted heavily to reviewing the available data sources, gathering previous regional seismic results and commencing a snythesis of gravity (free air and Bouguer) anomaly data and seismic refraction and reflection information. (The second year of this research project originally proposed for a three-year interval is being continued under NASA Grant NCC 5-19.)

To look for possible large-scale intraplate crustal features in eastern North America that may be associated with past or current tectonic structural elements, we analyzed 1° x 1° free-air anomaly data. This analysis included conventional and new techniques developed in this study for enhancement of structural boundarie.. Several large, regional blocks (> 500 km in lateral dimension) were identified that likely reflect deep crustal or upper mantle density differences. However, the correlation of regional seismicity with these large block structures is not strong enough to be compelling, although the major gravity anomaly patterns appear to follow major tectonic trends in the Eastern United States. Several smaller, distinct structural blocks are likely contained within each large block and these may be important to the tectonic interpretation. The details of this investigation are given in the Appendix. (Abraham Biadgelgne's M.S. paper).

We have also obtained and reviewed especially carefully the data from a comprehensive tectonic study of the Southern Appalachian Region recently conducted by the Tennessee Valley Authority (TVA) that includes gravity, seismic, remote sensing, aeromagnetic, and regional geologic

observations. These and other data that we have studied in detail suggest the presence of distinct crustal blocks that have lateral dimensions of the order of 50 km, and we are attempting to determine whether this characterization is typical of most areas in the EUS. Contained in the TVA study area is a major magnetic source body in S. Central Kentucky with associated strong gravity and seismic anomalies that extend upward to the base of the Paleozoic section; this feature and others that we can identify such as the Scranton gravity high are receiving special attention. In particular these major crustal anomalies are being investigated and modeled in more detail by R. Hawman in a M.S. thesis that is in progress. Details of his investigation will be reported under the continuation of this study (NASA Grant NCC 5-19).

During the past year we have also communicated frequently with NASA (Goddard) scientists to coordinate our work with the MAGSAT effort and we plan to continue this cooperative exchange. A vist to Penn State by Drs. Langel, Taylor, Allenby and Thomas was especially helpful in this regard.

Based on this initial year's study, future efforts should: (1) concentrate on obtaining more detailed information on the crustal structure in those areas exhibiting major (MAGSAT) regional magnetic anomalies, (2) refine models of the crustal structure in areas where seismic results (interpretations) are now lacking, and (3) combine our models with MAGSAT results. Crustal structure estimates from regional seismic networks that are now being operated in the EUS should be incorporated as well.

APPENDIX

The Pennsylvania State University

The Graduate School

Department of Geosciences

Third Derivative Analysis

of Gravity Anomalies

From Prismatic Sources

A Paper in

Geophysics

by

Abraham Biadgelgne

Submitted in Partial Fulfillment
of the Requirements
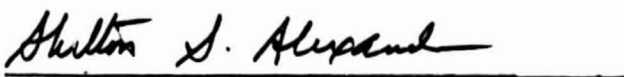for the Degree of

Master of Science

November 1979

The signatories below indicate that they have read and approved the thesis of Abraham Biadgelgne.

10/22/79

P. M. Lavin, Associate Professor of
Geophysics, Thesis Advisor

10/29/79

S. S. Alexander, Professor of
Geophysics, Head of Geophysics
Graduate Program.

22 Oct. 1979

E. K. Graham, Associate Professor of
Geophysics, Graduate Faculty Reader

October 29, 1979

C. A. Langston, Assistant Professor of
Geophysics, Graduate Faculty Reader

ABSTRACT

An interpretational technique based on the third vertical derivative of a gravity anomaly has been developed. The versatility and possible limitations of the method were evaluated by examining the response for two- and three-dimensional rectangular prisms with a wide range of sizes and depths. The effect of the interference of adjacent sources was also studied. It was demonstrated that for isolated prismatic models with thicknesses ranging from 0.2 to 20.0 sampling intervals, the third vertical derivative of the gravity anomaly outlines the top surface of the sources with error bounds of less than 8%. For cases in which the sources were in contact, the boundaries were delineated by well defined low or high trends. Moreover, the horizontal distance between the maxima and minima of the vertical derivatives gives an estimate of the depth to the source with error bounds of less than 9% if the thickness is less than two grid intervals. Depth estimation for sources in contact was complicated by the interference of the extrema of the derivatives. An approach for improving the results in such cases was proposed.

An attempt was then made to enhance some linear features in the most recent 1° by 1° gravity data for the central and eastern United States using the third vertical

derivative technique. Correlation of the inferred lineaments with some seismic trends and magnetic features assisted in outling some likely crustal blocks. The problem of the cuperposition of the effects of regional shallow and deep structures was discussed.

TABLE OF CONTENTS

LIST OF FIGURES

LIST OF FIGURES - cont.

LIST OF TABLES

ACKNOWLEDGEMENT

CHAPTER I

INTRODUCTION

Quantitative interpretation of data collected in a gravity or magnetic field survey involves investigating various types of models that will best fit the observed anomaly and the known geology of the region of interest. For this reason, there is no paucity of papers discussing techniques for evaluating the field due to different model sources (e.g., Henderson and Zeitz, 1948; Vacquier, 1958; Battacharyya, 1964, 1966). From among such models, the rectangular block-shaped body has found the most widespread applications in the interpretation of potential field data. The popularity of the model arises from its versatility in representing a wide variety of geological structures and from its utility as a building block for complex mass distributions. Looking into the future, one expects the model to gain more importance as satellite determination of the earth's gravity and magnetic field increases the desirability and the feasibility of studying major crustal structures.

In the past, various qualitative and quantitative interpretational techniques have been developed to assist in determining the physical parameters of field sources. Of all these, a method that has been used extensively to interpret aeromagnetic data from various geological

provinces is the one first developed by Vacquier et al. (1958) and later extended by Battacharyya (1964, 1966) and Jain, et al. (1974). Vacquier, et al (1958) conducted detailed model studies and showed that the zero contour of the second vertical derivative of the magnetic field closely outlines the top surface of a vertically sided, isolated prismatic model with infinite thickness and vertical magnetization. Moreover, Jain, et al. (1974) showed that the horizontal distance between the plotted maxima and minima of the derivatives gives a reasonably accurate estimate of the depth to the source.

Standard interpretational techniques have been applied for the gravity case. However, in the past, no attempt has been made to apply the Vacquier, et al. (1958) approach. Hence, in this paper it will be shown that the general procedure of determining the horizontal dimensions and the depth of a prismatic source is also applicable to gravity, since Poisson's relation implies that the second vertical derivative of the magnetic field of a source is equivalent to the third vertical derivative of its gravity field, provided certain basic assumptions discussed later are met. Two major differences between the gravity and the magnetic problems are expected to affect the results of the gravity case. In magnetics, the prismatic models are assumed to have infinite thicknesses. This allows one to deal only with a sheet of monopoles at the top surface. However, in

gravity, there is a continuous distribution of density with depth which requires the model be limited to a finite thickness in order to avoid a singularity. Thus, the effect of finite thickness on the position of the zero contour and on the estimation of depth must be determined. An important advantage of using gravity data over magnetic data is that there is no need to correct field data for inclined field direction, i.e., the gravity field is already "reduced to the pole." The implication of these basic factors will be explored in detail in later sections for both two- and three-dimensional model·. For the sake of simplicity, most of the analysis will be conducted in the wavenumber domain.

Finally, the interpretational technique will be applied to the most recent 1° by 1° free-air gravity data of the eastern and central United States prepared by Rapp(1978). The main intent of this study will be to enhance some major linear features suggested by the field data. Some basic limitations of the data set that make the final outcome of this aspect of the investigation preliminary in nature will also be addressed.

CHAPTER II

THEORY

The theoretical framework for the interpretational technique developed in this paper will be presented herein. The general approach will be to begin with a review of the interpretational scheme used in magnetics, and then to invoke Poisson's theorem to show the nature of the operation for gravity data. This will be followed by a discussion on the gravity effects of a rectangular prismatic model with finite thickness. An analysis of both the continuous and discrete forms of the vertical derivative operators will also be presented in the wavenumber domain for later use.

Magnetic Theory and Its Applications

Vacquier, et al. (1958) have shown that for bottomless rectangular prisms that have great areal extent compared to their depth of burial, the zero contour for the second vertical derivative of the magnetic field closely follows the outlines of the top surface of an isolated body. The theoretical framework for this concept is based on the assumption that the anomalous field results solely from induction in the earth's magnetic field and that the field is nearly vertical. However, experimental work on rock magnetism by several investigators (Green, 1960; Ross and Lavin, 1966; and Battacharyya, 1964) has demonstrated that

remanent magnetization is commonly present and may even dominate the induced magnetization. Despite this restriction, a wide application of this rather simple technique over diverse geological provinces has lead to significant results (Jain et al., 1974; Bhattacharyya, 1966; Zeitz et al., 1967). In cases where a relatively strong remanent magnetization exists at an angle to the earth's field, or where the dip of the magnetization vector is too low, the contours would be skewed to one end of the model and the inflection points would not mark the edges of the model (Zeitz and Andreasen, 1967). For such cases, the asymmetry in the contours may be improved by reduction to the pole if the magnetization direction is known.

The other main information obtained from the vertical derivative operator, in magnetics, is the estimation of the depth to the top of the prismatic source. The horizontal distance between the maxima and minima of the second vertical derivative, R, has been related to the depth of the source, D_s, through theoretical studies and detailed empirical observations. Jain et al. (1974) have shown that R varies in almost direct proportion to D_s, or

$$D_s = CR \qquad (1)$$

where C is a constant that ranges from 1.2 for very narrow or very wide bodies to about 1.4 for bodies whose width is double the depth. In general, taking the value 1.3 for C limits the percentage errors in depth estimation to within

10%. Once again, if the reduction to the pole is
incomplete, due to a lack of information on the direction of
magnetization or due to inadequate data processing, the
value of C may be as high as 1.5 leading to erroneous depth
determinations (Jain, 1974). It has also been observed that
for cases in which the distance between different sources is
roughly equal to or less than the depth of burial, the
technique provides less reliable depth estimates.

Poisson's Theorem and Its Applications

The Newtonian or gravitational potential and the
magnetic dipolar potential are related by a simple equation
provided the restrictive assumptions discussed below are
met. Suppose the mass of a body that fills a volume, V, has
a continuously distributed dipole moment per unit volume,
$I\vec{t}$, where I is its magnitude and $\vec{t}$ is a unit vector in the
direction of magnetization. Then, the magnetic potential,
$A(\vec{r})$, at an arbitrary point, S, outside the body (Figure 1A)
is given by

$$A(\vec{r}) = - I \frac{\partial}{\partial t} \int \frac{dV}{|\vec{t} - \vec{r}_o|} \quad . \tag{2}$$

Similarly, the gravitational potential due to a continuous
mass of density, D, at the same exterior point, S, is given
by

$$U(\vec{r}) = - QD \int \frac{dV}{|\vec{r} - \vec{r}_o|} \quad , \tag{3}$$

A. Spatial Domain

$$u = p\cos(\phi)$$
$$v = p\sin(\phi)$$
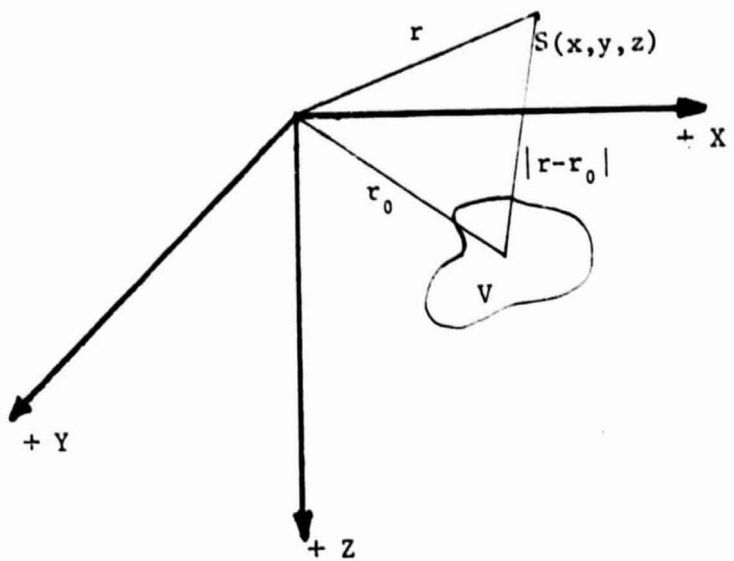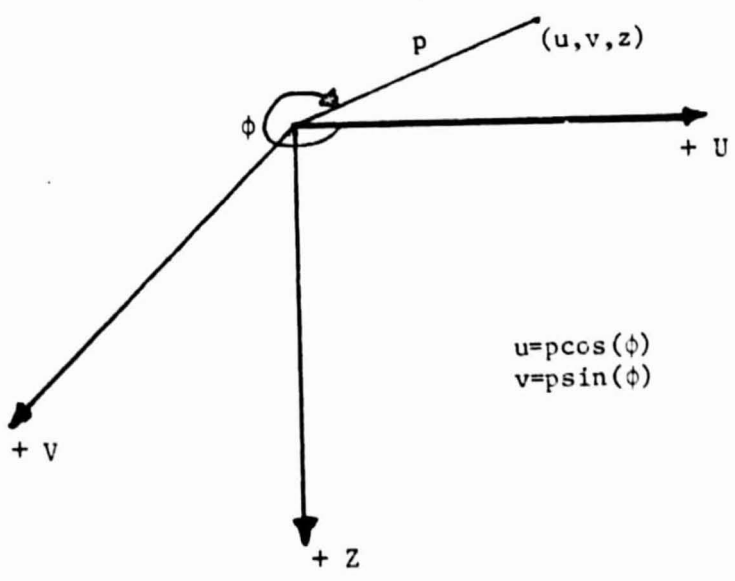
B. Wavenumber Domain

Figure 1. Coordinate System.

where Q is the Gravitational Constant (6.67 x 10^{-8} cgs units). Assuming that the density, D, is uniform and the magnetization, I, is uniform both in magnitude and direction over the same volume, V, t e geometric factor of Equations 2 and 3 may be equated giving

$$A(\vec{r}) = \frac{I}{Q} \frac{}{D} \frac{\partial}{\partial t} U(\vec{r}) \qquad . \qquad (4)$$

The above equation, which is attributed to Poisson (1826), implies that all the properties of the magnetic potential of an anomalous body are derivable from its gravitational potential or vice versa, provided the basic assumptions are met. For cases in which the vertical component of the magnetic field are considered, Equation 4 may be differentiated to obtain

$$H_z = \frac{I}{Q \ D} \frac{\partial}{\partial t} g_z \qquad , \qquad (5)$$

where H_z and g_z are the vertical components of the magnetic and gravity fields, respectively.

Equations 4 and 5 have been widely applied in the analysis of local and regional anomalies. Garland (195ib) used the relation in transforming the Crow Lake gravity anomaly in the Canadian Shield into a magnetic anomaly, and demonstrated that the source was non-uniformily magnetized. Lundback (1956), Ross and Lavin (1966), and Robinson (1971)

have applied various versions of Poisson's relation to determine the direction of magnetization for two- and three-dimensional bodies by the transformation of gravity or magnetic fields. Recently, a numerical approach that employs least-square inversion of gravity and magnetic data in the wave number domain has been successfully used to determine the ratio I/D, and the direction of magnetization (Cordell and Taylor, 1971). Kanasewich and Agarwal (1970) have also applied the theorem in the wavenumber domain to compare gravity data measured over a large area with the corresponding magnetic field data reduced to the pole.

In the present study, Poisson's relation is used to relate higher order vertical derivatives of gravity and magnetic fields. Suppose that the field source is vertically magnetized, or that it is reduced to the pole. Then, Equation 5 becomes

$$H_z = \frac{I}{Q\,D} \frac{\partial}{\partial z} g_z \quad . \tag{6}$$

Differentiating twice with respect to z gives

$$\frac{\partial^2}{\partial z^2} H_z = \frac{I}{Q\,D} \frac{\partial^3}{\partial z^3} g_z \quad . \tag{7}$$

Equation 7 shows the second vertical derivative of a magnetic field corresponds to the third vertical derivative of the gravity field. Thus, one can extend the magnetic

analysis procedure of Vacquier, et al. (1958) and Jain, et al. (1974) to gravity anomalies by employing the third vertical derivative of the field.

Gravitational Anomaly of Rectangular Prism

A right rectangular prism with sides parallel to the coordinate axis, at depth H below the surface of observation is shown in Figure 2. The derivation of a closed expression for the vertical component of the gravitation attraction at an arbitrary point, S(x,y,z), outside of or on the boundary of the prism was given by Nagy (1966). Through a simple transformation of his coordinate system, the general equation for the field value at an arbitrary point becomes

$$
g_z = QD \left|\left|\left| (\alpha - x)\ln(\beta - y + R) + (\beta - y)\ln(\alpha - x + R) \right.\right.\right.
$$
$$
\left.\left.\left. - (\gamma - z)\arcsin \frac{(\beta - y)^2 + (\gamma - z)^2 + (\beta - y)^2 R}{(\beta - y + R)(\beta - y)^2 + (\gamma - z)^2} \right|\right|\right| , \quad (8)
$$

where the variables are evaluated from $X_c - A$ to $X_c + A$ for α, from $Y_c - B$ to $Y_c + B$ for β and from H to H + T for γ (Figure 2).

The complexity of the space-domain expression limits its usefulness in interpretational schemes for all practical purposes. All the parameters of the prism are contained in coupled terms and extraction of any of them appears rather difficult. Moreover, the analytic evaluation of the third vertical derivative in the spatial domain would be very

$$R^2 = (\alpha - x)^2 + (\beta - y)^2 + (\gamma - z)^2$$

$\bullet$ S(x,y,z)

2A

2B

T

(x_c, y_c, H)

dV
(α, β, γ)

+ X

+ Y

+ Z
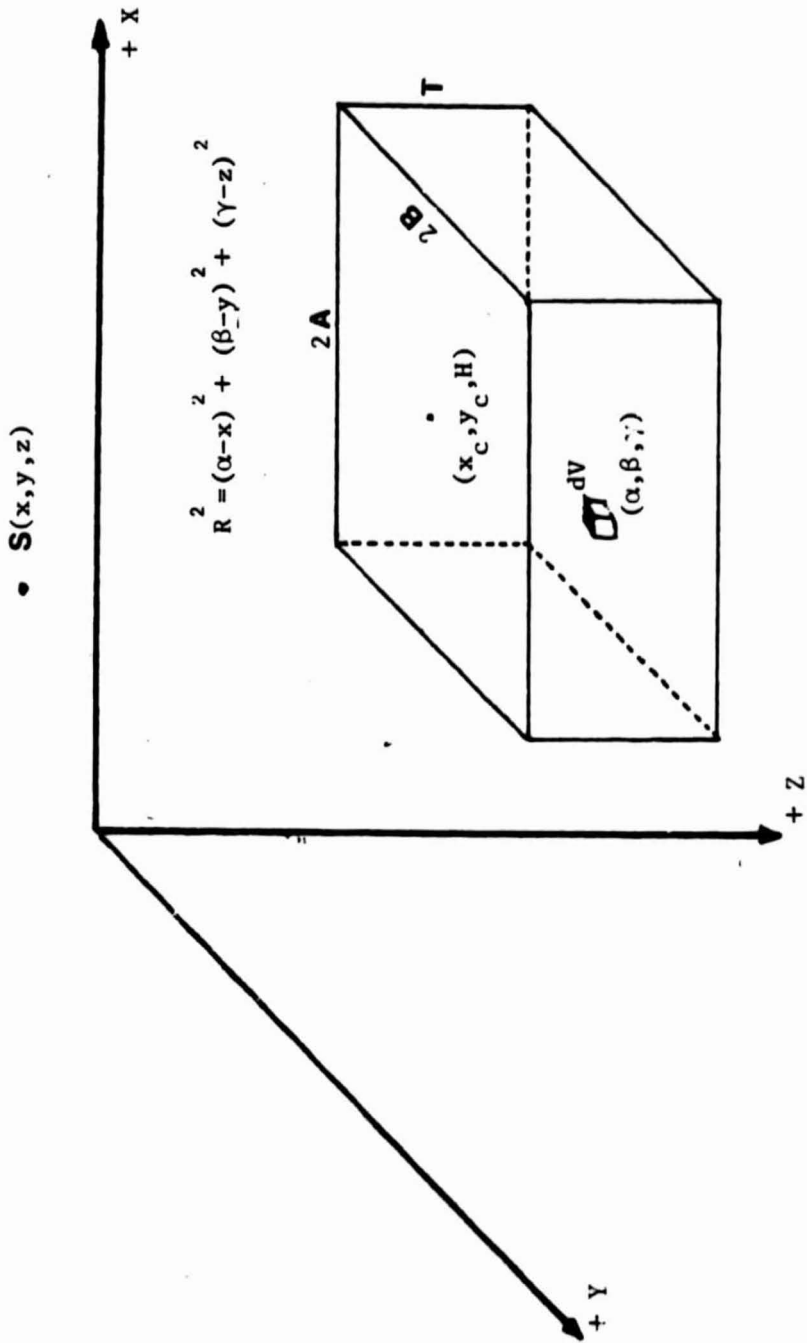
Figure 2. Geometry of a rectangular prism.

cumbersome at best. The first vertical derivative alone involves over ten terms, and it is not difficult to imagine how intractable the third vertical derivative would be.

Alternatively, the gravity effect may be represented by its Fourier transform given by

$$G(u,v) = \int_{-\infty}^{\infty} g(x,y) \exp(-i(ux + vy)) \, dx \, dy \quad , \quad (9)$$

where

$$g(x,y) = 1/(4\pi^2) \int_{-\infty}^{\infty} G(u,v) \exp(iux + ivy) \, dx \, dy \quad , \quad (10)$$

and u and v are wavenumbers in radians per unit length in the X and Y directions, respectively.

It is worthwhile to note that to have a definite Fourier transform, in strict mathematical sense, a function needs to be absolutely integrable over the X-Y plane. This requires the function to go to zero over large values of X and Y. However, the gravity field of anomalous sources does not vanish over the surface of observation, and, in fact, theoretically, it extends to infinity. To overcome this mathematical difficulty, one must assume that the field will be defined over a large, but finite area of the coordinate plane and that it becomes zero outside this domain. A method for reducing truncation effects that arise from such finiteness of the surface of observation will be addressed in the data processing section of the next chapter.

Carroll (1973) showed that the spectrum for a rectangular prismatic model with finite thickness is given by

$$G(u,v) = \frac{2\pi QM}{T\ p} \exp(-Hp)\ (1 - \exp(-Tp))\ \text{sinc}(Au)$$

$$\text{sinc}(Bv)\ \exp(-ix_c u)\ \exp(-iy_c v) \qquad (11)$$

where M is the total mass and $p^2 = u^2 + v^2$ (Figure 1B). The wavenumber expression of the gravity field is simpler to analyze since the parameters are now uncoupled into separate terms. The term $\exp(-Hp)$ represents the depth term, $(1 - \exp(-Tp))/Tp$ represents the thickness term, and the sinc functions, $\text{sinc}(Au)$ and $\text{sinc}(Bv)$ represent the width terms. It is also noted that Equation 11 may be modified further to accomodate two-dimensional problems, by assuming the gravity field to be constant along one of the axes. If, for instance, the field is constant parallel to the Y axis, the v dependence in Equation 11 will drop out, leaving the spectrum for a rectangular parallelpiped extended along the Y axis to infinity (Carroll, 1973), or

$$G(u,v) = \frac{2\pi QM_2}{T\ |u|} \exp(-H|u|)(1 - \exp(-T|u|))$$

$$|\text{sinc}(Au)|\ \delta(v) \qquad , \qquad (12)$$

where M_2 is the mass per unit length of the source and $\delta(v)$ is the delta function.

Discrete Form of the Nth Vertical Derivative

The vertical derivative of order n has a wavenumber response given by (Agarwal, 1972)

$$F^n(u, v) = (u^2 + v^2)^{n/2} . \qquad (13)$$

In particular, for our purpose, the ideal third vertical derivative operator has the form

$$F^3(u, v) = (u^2 + v^2)^{3/2} . \qquad (14)$$

Hence, the third vertical derivative of a gravity field can be easily obtained by multiplying $G(u, v)$ by $F^3(u, v)$ as shown below

$$G^3(u, v) = G(u, v) \quad F^3(u, v) , \qquad (15)$$

and then inverse Fourier transforming the result. The simplicity of the approach in the wavenumber domain stands in clear contrast to the rather intractable alternative of the analytical evaluation of the derivative in the spatial domain.

The gravity and magnetic effects that observed field data represent are, in reality, continuous functions, while, in practice, one often only knows these functions at points of intersection of a grid. This requires that we discretize the smooth and continuous vertical derivative operator, $F^3(u, v)$. If we have N data points in the X-direction and M data points in the Y-direction, the sampling intervals in the wavenumber domain, in cycles per data interval will be

$$\Delta k_1 = 1/N \quad \text{and} \quad \Delta k_2 = 1/M \qquad . \qquad (16)$$

Equation 14 then becomes

$$D^3(k_1, k_2) = ((\frac{2\pi k_1}{N})^2 + (\frac{2\pi k_2}{M})^2)^{3/2}, \qquad (17)$$

where k_1 and k_2 are the integers 0, 1, 2, ... For the discrete case Equation 15 may be rewritten as

$$G^3(k_1, k_2) = G(k_1, k_2) \ D^3(k_1, k_2) \ . \qquad (18)$$

It is important to note that the derivatives (Equation 17) are independent of the internal mass distribution and can be computed unambiguously for any observed surface data. Moreover, the form of the vertical derivative operator shows the tendency to amplify high wavenumber anomalies and observational errors relative to broad features in the surface field. It is, thus, imperative to make a detailed inspection of the spectrum of the measured anomaly, and then decide which wavenumber range should be operated on and which parts of the Fourier spectrum should be suppressed, thereby gaining full control over the output of the derivative operator.

Determination of Width and Depth Parameters

In the previous sections we have shown that Poisson's theorem justifies an approach for gravity field analysis equivalent to the magnetic interpretational technique. This implies that the zero contour of the third vertical derivative of a gravity field will closely outline the top surface of a rectangular prism with finite thickness. In cases where a continuous distribution of sources is encountered, the zero contours would be expected to delineate the boundaries between the sources. In fact, one apparent advantage in gravity interpretation is that the anomaly is "naturally" reduced to the pole. Hence, there is no problem of the zero-contour being skewed to one edge of the prismatic models, as would be the case in magnetics when the source is not vertically magnetized. On the other hand, care must be taken in specifying the thickness of the models. In magnetics, the effect of the north and south poles of the magnetization vectors of a vertically-sided prismatic model cancel each other except for the ones at its top and bottom surfaces. This implies that the vertical component of the magnetic intensity at any point of observation is proportional to the difference of the solid angles subtended by the top and bottom surfaces, respectively. Hence, in the case of bottomless rectangular blocks, one has to consider only the effect of a sheet of monopoles at the top. However, in gravity, there is a

continuous distribution of density with depth, and extending the thickness to infinity will lead to a singularity. This requires that, unlike the approaches followed in magnetics (Vacquier, et al., 1958; Brattacheryya, 1964, 1966; Jain, 1974), the gravity investigation must be restricted to prismatic models with finite thicknesses. Hence, one must study the relation of thickness to the position of the zero contour and determine the range of thicknesses over which the method works.

Another major application of the vertical derivative scheme is based on the relationship of the depth to the top of the source and the horizontal distance between the maxima and minima of the second vertical derivative of the magnetic field as shown in Equation 1 (Jain, et al., 1974). It should also be noted that Equation 7 gives a linear relationship between the second vertical derivative of a magnetic field and the third vertical derivative of a corresponding gravity field. Hence, the method for estimating the depth to the source is readily transferable to the interpretation of an anomaly due to an isolated gravity source, provided the implications of the restrictions put on the thickness as discussed above are respected.

CHAPTER III

PROCESSING AND INTERPRETATION ON MODEL DATA

To examine the utility of the interpretational technique formulated in Chapter II, the gravity anomalies of several numerical models and their third vertical derivatives were studied using various data processing schemes. For the sake of simplicity and ease of study, most of the detailed analysis was focused on two-dimensional rectangular parallelepipeds with finite thicknesses. This was supplemented by a limited consideration of three-dimensional models, to show the effect of having two or more models that are in contact or well isolated. The overall reliability and possible limitations of the method were also evaluated. Several of the more interesting two- and three-dimensional model studies are described herein.

Data Processing

The gravity anomaly for a right rectangular prism of finite thickness was generated using computer programs based on the Talawani algorithms (Talawani, 1965; Talawani and Heirtzler, 1964). The anomaly was then fast-Fourier transformed (Cooley and Tukey, 1965) for processing with the discrete form of the third vertical derivative operator (Equation 17).

A problem was encountered early in the study brought about by the basic assumption that the field becomes zero outside the area of observation. Such data-set truncation in the spatial domain results in high wavenumber oscillations in the wavenumber domain. To avoid this undesirable phenomenon, a Hanning window was found to be the most suitable pre-transform filter. The form of the window used for a two-dimensional data set is

$$W(x,y) = \frac{1}{4} (1 + \cos \frac{\pi x}{N}) (1 + \cos \frac{\pi y}{M}) \tag{19}$$

$$\text{for } x < N \text{ and } y < M ,$$

where N and M are the array sizes of the gravity field data in the X and Y direction, respectively. For profile data, one of the variables (X or Y) is set to zero.

Another problem encountered early in the project was the sensitivity of the vertical derivative operator to the selection of grid spacing. Model profiles were generated with even spatial sampling intervals of different lengths. In general, the results demonstrate that the finer the grid spacing, the more accurate the computed values of the horizontal dimension and the depth of the prismatic models. On the other hand, it is important to note that the superimposed grid acts as a filter that retains anomalies pertaining to sources of certain wavelengths. However, in some geophysical studies local or shallow anomalies are of minor or no interest and should be eliminated. Hence, in

practice, there is a need to use a grid spacing which is commensurate with the structural features being studied provided alaising of the data-set is avoided. For our particular purpose, a sampling interval of about 0.2 times the width of the numerical models gave adequate results in outlining the top surface of the sources,while a value of 0.1 was required for estimating their depth of burial. These values result in oversampled data. In cases where coarser grid spacings were employed, interpolation to finer spacing using the bi-cubic spline interpolation in the spatial domain and padding with zeroes in the wavenumber domain were found to be particularly useful in improving the results.

Delineation of Block Boundaries

The effectiveness of the zero contour of the third vertical derivative in outlining the edges of an isolated source or in delineating the lithologic boundaries of continuously distributed sources are influenced by the physical parameters of the bodies. Detailed and systematic empirical investigations were carried out to determine possible restrictions introduced by these factors. Some of the most significant results will be discussed below.

One of the prerequisites for carrying out a field survey or a model study is selecting an appropriate sampling scheme. In field applications, the grid spacing would be

set depending on the data coverage desired and/or the logistics of the date acquisition process. In model studies, they are selected to give reasonably accurate results without being too fine for practical applications. The proper grid interval selected on this basis has been discussed in the data processing section. In the subsequent sections, the procedure followed is to use an adequate sampling interval (0.2 or 0.1 times the width) for a particular model and then to vary the physical parameters, keeping the grid spacing fixed. In this manner, one determines the range of parameters that will be covered for a given condition without introducing serious errors. The standard model used for this purpose has a width equal to 12.0 sampling intervals. The parameters were varied over ranges consistent with the nature of the gravity field data expected in the next chapter. It should also be noted that, from now on, the grid spacing is the unit of measurement when it is not specified otherwise.

Two-Dimensional Models

Figure 3 illustrates a typical gravity anomaly and its third vertical derivative for a two-dimensional rectangular parallelpiped. The location of the maxima and minima of the derivative are indicated by A' and B', respectively. The position of the reversal of sign in the values of the derivative is indicated by C'. This corresponds to the zero contour in the three-dimensional case.
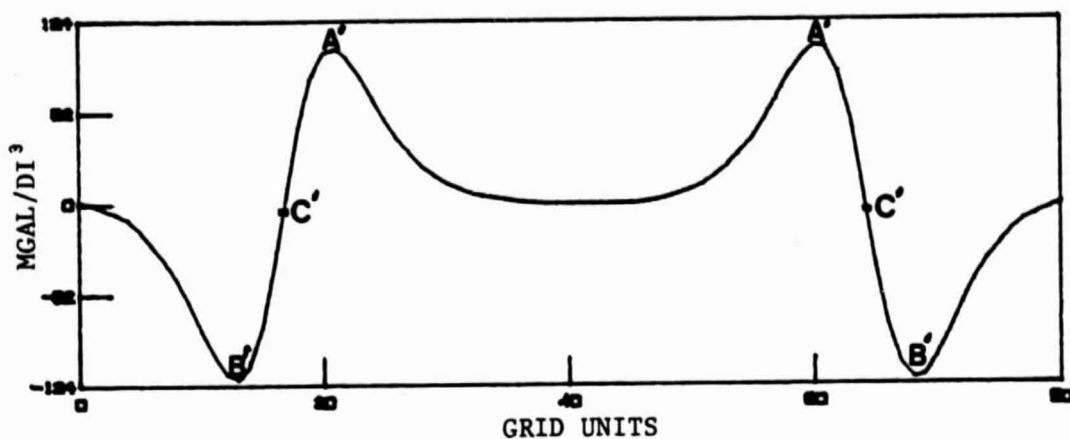
C. Third vertical derivative of the field
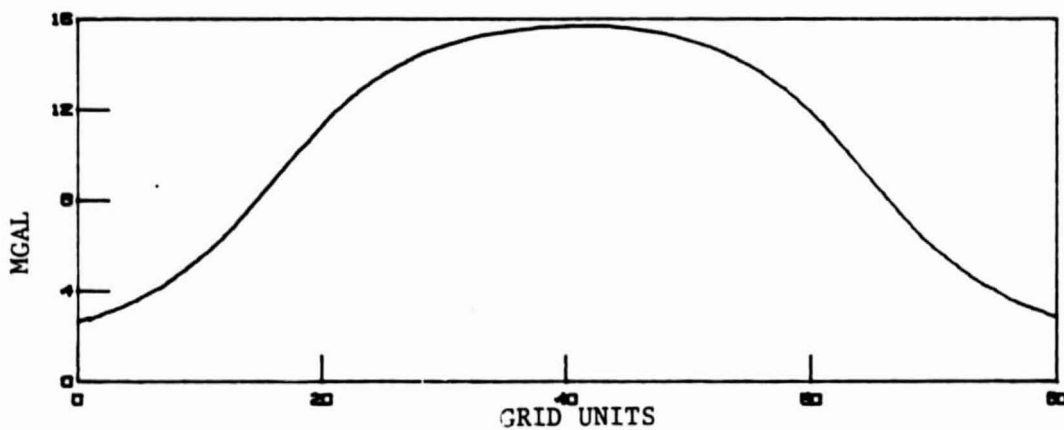
B. Gravity anomaly
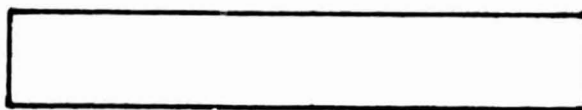
A. Model geometry.

Figure 3. The gravity anomaly and third vertical derivative for a rectangular prism.

Table 1 gives a sample of interpretational results showing the effects of thickness on width estimations. A two-dimensional rectangular parallelpiped with a width equal to 12.0 was employed. The depth was kept fixed at 2.0, while the thickness varied from 0.2 to 20.0. The data indicates that accurate determinations of width with error bounds of less than 2.2% are to be expected over all the range of thicknesses considered. A slight increase in the differences between actual and predicted width is noticed as the thickness increases by two orders of magnitude. It should be noted that, since there is a continuous distribution of density with depth, increasing the thickness amounts to adding some more mass to its deep end. Hence, in the limit as the thickness goes to infinity one would be faced with a singularity. This would, necessarily, lead to a slowly increasing inaccuracy in the results.

Table 2 shows the effect of using a fixed grid interval and profile length that were found adequate for a model width equal to 12.0 for models of other widths. The depth for all models was 2.0, and the range of width considered varied from 2.0 to 24.0. The thickness was kept constant at 4.0. Truncation effects introduced as the models extend closer to the border probably contributed to the slightly higher errors for wider models, though the Hanning window has greatly reduced such effects. The narrower models, on the other hand, have been greatly

TABLE 1

EFFECT OF THICKNESS ON WIDTH ESTIMATION

Thickness (sampling unit)	Estimated Width (sampling unit)	Percentage Error
0.2	11.88	-0.7
0.4	11.86	-1.2
0.6	11.84	-1.3
0.8	11.84	-1.3
1.0	11.82	-1.5
1.2	11.82	-1.5
1.6	11.80	-1.6
2.0	11.80	-1.6
4.0	11.76	-2.0
8.0	11.74	-2.2
12.0	11.74	-2.2
16.0	11.74	-2.2
20.0	11.74	-2.2

affected. The smallest model presented shows an error of 30%. This primarily reflects the effect of inadequate sampling of the data for the particular case. The same analysis was repeated for a range of thicknesses extending from 0.2 to 20.0 and a similar trend in percentage errors was observed. The only difference was that the thickness effect makes the overall errors slightly higher as was the case in Table 1.

Several models were evaluated to examine the influence of the depth parameter in outlining the top surface (Table 3).

Within the range of practical interest for local and regional studies, the results are reasonably accurate. As we probe for deeper sources, the inaccuracy in the predicted

TABLE 2

WIDTH ESTIMATIONS FOR FIXED SAMPLING INTERVAL

Width (sampling unit)	Estimated Width (sampling unit)	Percentage Error
2.0	2.60	+30.0*
4.0	4.24	+ 6.0
6.0	5.86	- 2.3
12.0	11.76	- 2.0
18.0	17.60	- 2.2
24.0	23.42	- 2.4

* curve very oscillatory

values increases slightly. In fact, the errors become even larger when the effect of width and thickness shown in Tables 1 and 2 are included with the depth effect. This would be especially true for very narrow sources that are extremely thick. Hence, once again, it is noted that the extremely narrow sources suffer more than the extended ones. This is, perhaps, reflective of the nature of the depth term in Equation 12, together with the problem of inadequate sampling discussed before. The data spectrum in Equation 12 falls off as $\exp(-H|u|)$ with increasing value of H. Thus, the depth factor acts as a low-pass filter.

It should be noted that the results given in the three tables cover a wide range of depth, width and thickness that are quite realistic. If, for instance, a grid interval in a field survey is assumed to be 10 km, the range of

TABLE 3

EFFECT OF DEPTH ON WIDTH ESTIMATION

Depth (sampling unit)	Estimated Width (sampling unit)	Percetage Error
1.0	11.94*	-0.5%
2.0	11.80	-1.7%
3.0	11.60	-3.3%
4.0	11.44	-3.3%
5.0	11.26	-6.2%
6.0	11.10*	-7.5%
7.0	11.04*	-8.0%

* curve very oscillatory

thicknesses (Table 1) ranges from 2 km to 200 km. The range of widths extends from 20 km to 240 km, while the depth varies from 10 km to 70 km. Similar range estimations are plausible for other grid intervals depending on the field survey desired. It is also noted that for most of the noise-free data that has been considered, the range of errors is less than 8 percent. These error values indicate that the results are reasonably accurate for practical purposes.

Three-Dimensional Models

To illustrate the versatility of the interpretational technique in outlining isolated gravity sources, and in delineating lithologic boundaries, several empirical models

were run using a three-dimensional rectangular prism with finite thickness as the basic model. Some of the more interesting results are discussed below.

The effect of truncation was studied by processing a segment of the anomaly generated for a rectangular prism of finite thickness(Figure 4). Several pre-transform filters were tested in an attempt to smooth the data spectrum and prevent spectral leakage. However, the output of the vertical derivative operator persistently showed some instability at the truncated end. To circumvent the problem, the derivative operator was designed in the spatial domain. The set of weights were derived by inverse-Fourier transforming the wavenumber expression of the third vertical derivative operator and then truncating it into a set of 7 by 7 coefficients by using a symmetric Hanning window (Equation 19). The wavenumber response of the filter is shown in Figure 5. It is noted that over a wide range of wavenumbers the behavior of the amplitude response is circularly symmetric as it would be with the ideal case. A reversal of the curvature of high wavenumber contours occurs for wavenumbers greater than about 0.4 cycles per data interval (cycles/di). This effect, which is also observed in several of the wavenumber responses of operators reported in the geophysical literature (Henderson, 1960; Elkins, 1951; Fuller, 1967) is primarily a result of the loss of circular symmetry caused by specifying the discrete weights
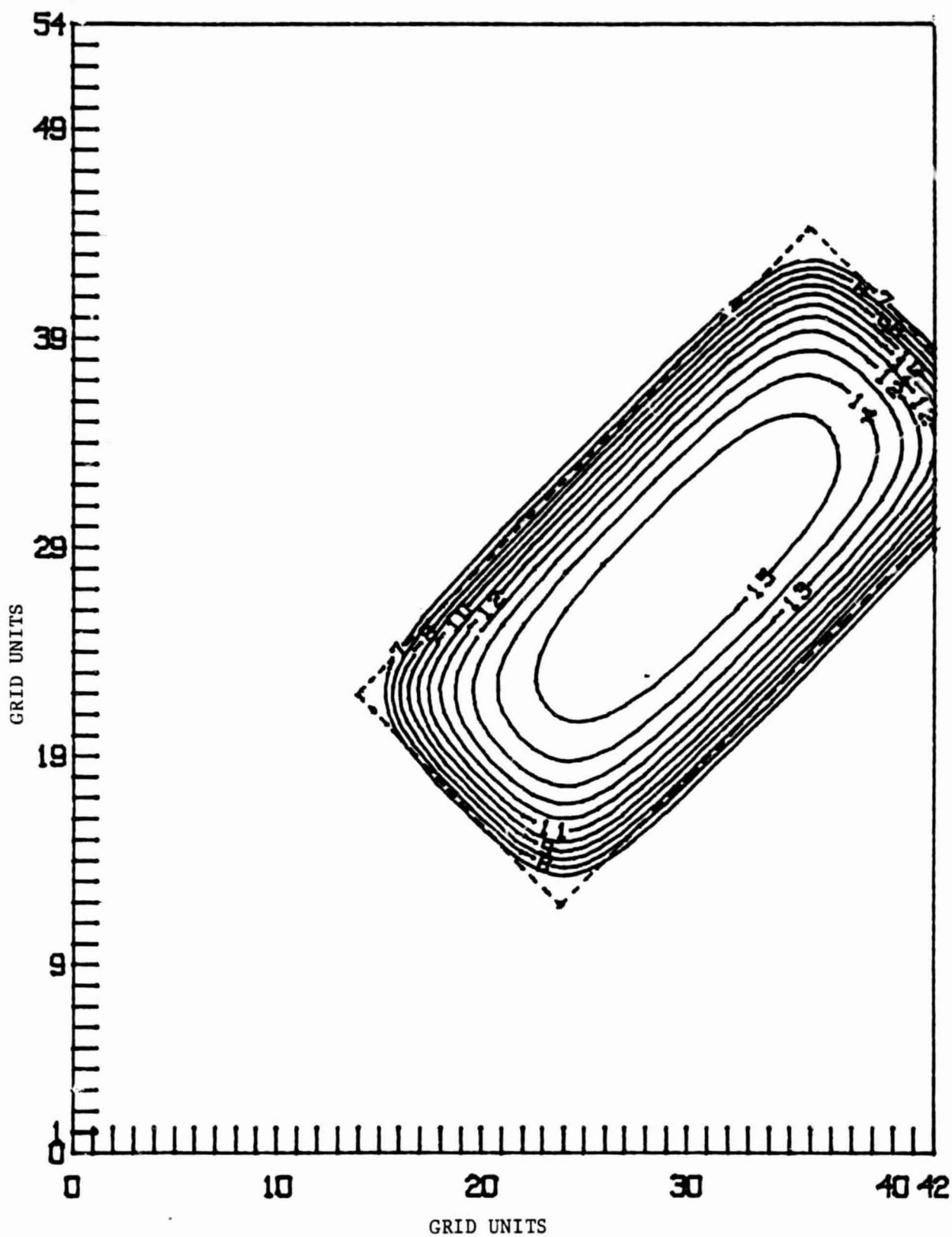
Figure 4. A segment of the gravity anomaly generated for a
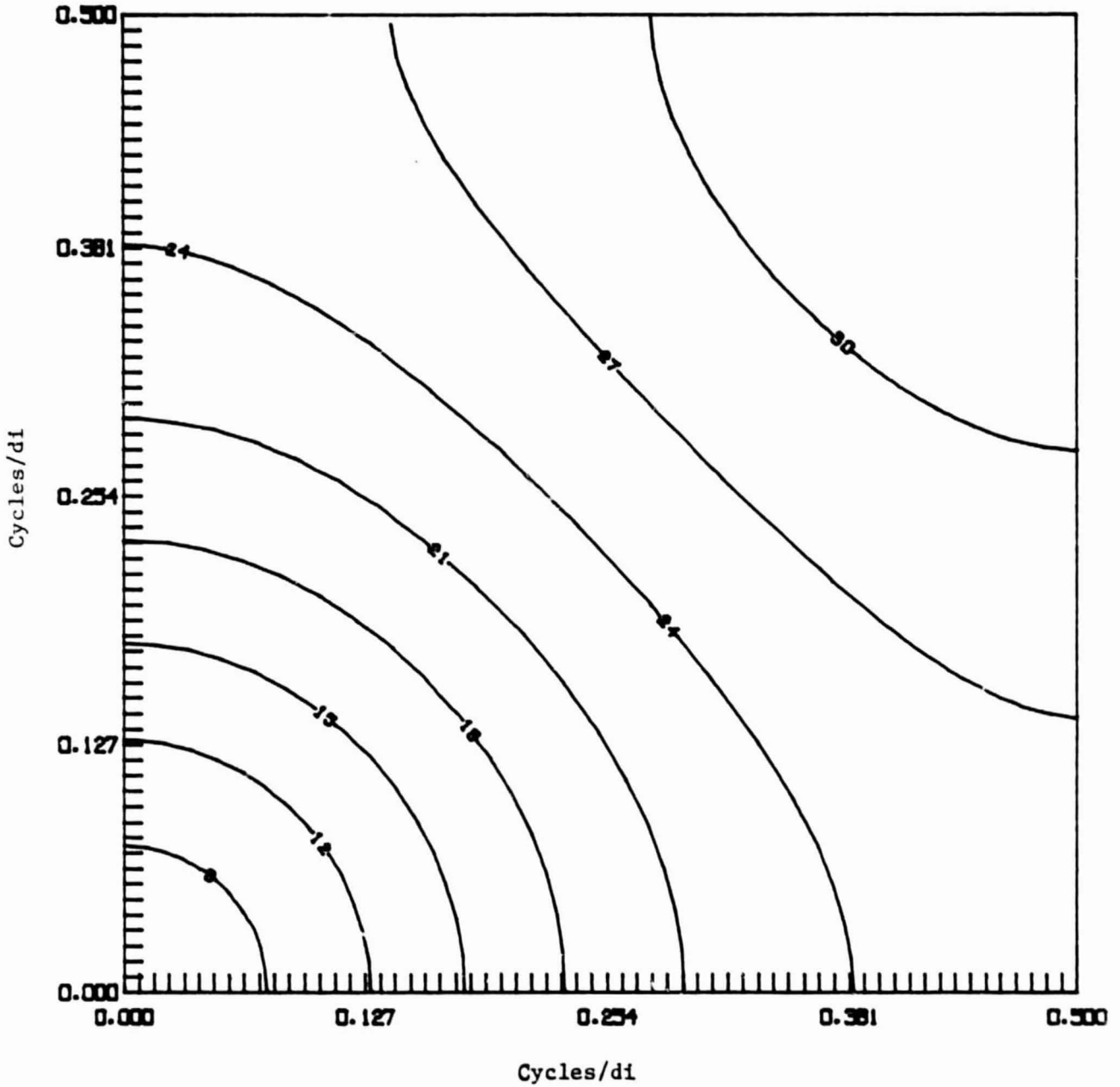three-dimensional rectangular prism (contour intervals in mgals).

Figure 5. The amplitude response of the third vertical derivative operator designed in the spatial domain. (contours interval = 3 db)

on a square grid (Fuller, 1967). However, most of the energy content of the data is concentrated below about 0.1 cycles/di, and should not be affected by the asymmetry. Considerable improvement in the accuracy of the output was achieved by convolving the set of coefficients with the gravity anomaly (Figure 6). The resolution of the upper corner of the body and the delineation of the truncated end is rather striking. It should also be noted that the loss of data around the edges during the convolution process has caused the origin to be shifted by 3 grid units both in the X and Y direction.

Figure 7 gives the gravity anomaly of an isolated prismatic model with its position indicated by dashed lines. The model has a length of 21.0, a width of 14.0 and a thickness of 1.0. The upper surface is located at a depth of 3.0. Although the anomaly inflection line roughly corresponds to the vertical boundaries of the prism, the third vertical derivative of the anomaly enhances this information considerably (Figure 8). The maxima and minima flank the zero contour that marks the edges of the body with reasonable accuracy. Unlike in magnetics, where there is a preferential shift of the contours towards one of the poles, depending on the direction of magnetization, the zero contour for gravity data shows symmetry around the body.

The anomaly of two prisms in contact is shown in Figure 9. Dashed lines indicate the position of the models. They
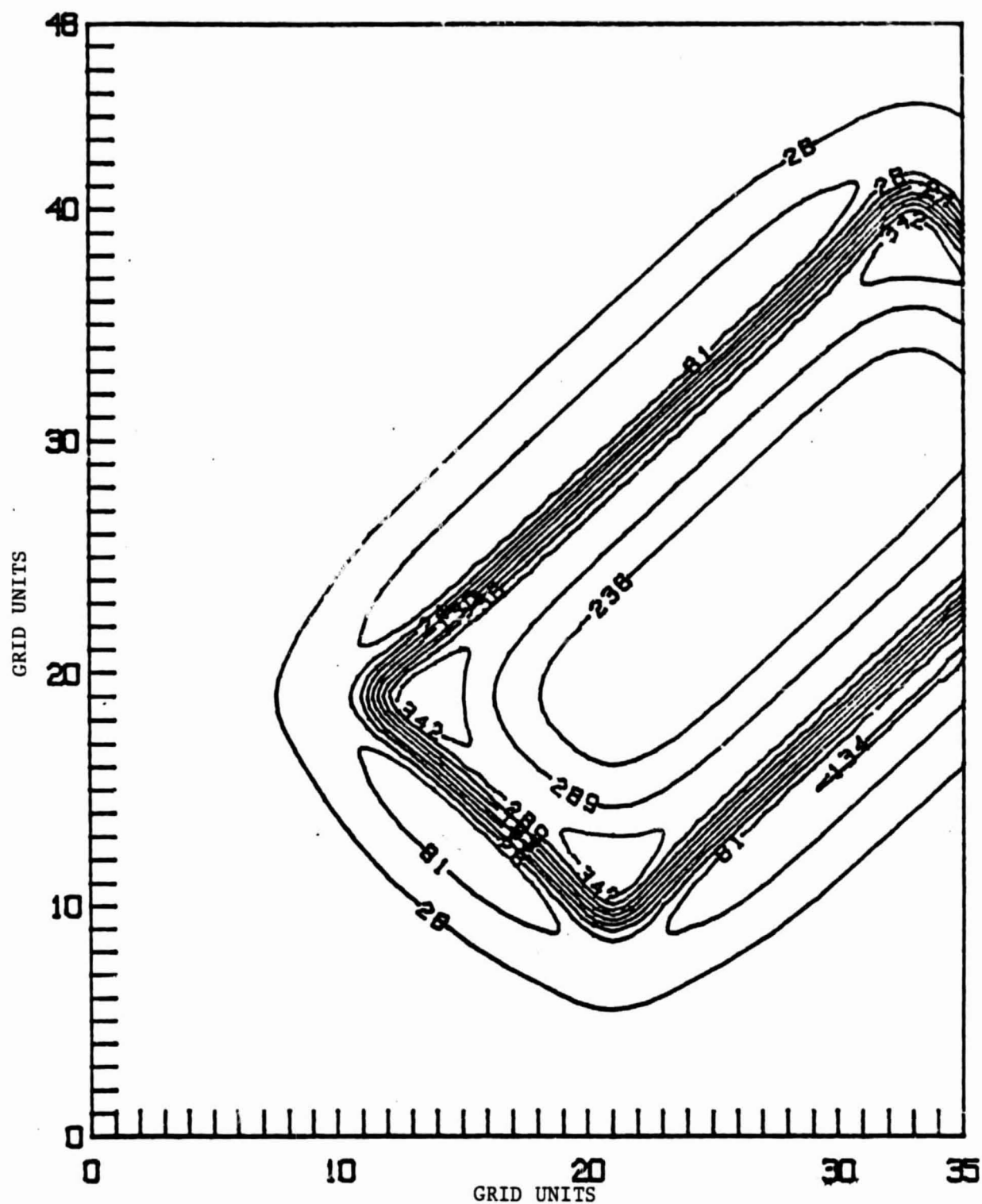
Figure 6. The third vertical derivative of a segment of a gravity anomaly generated for a three-dimensional rectangular prism (contour interval in mgals/di³)

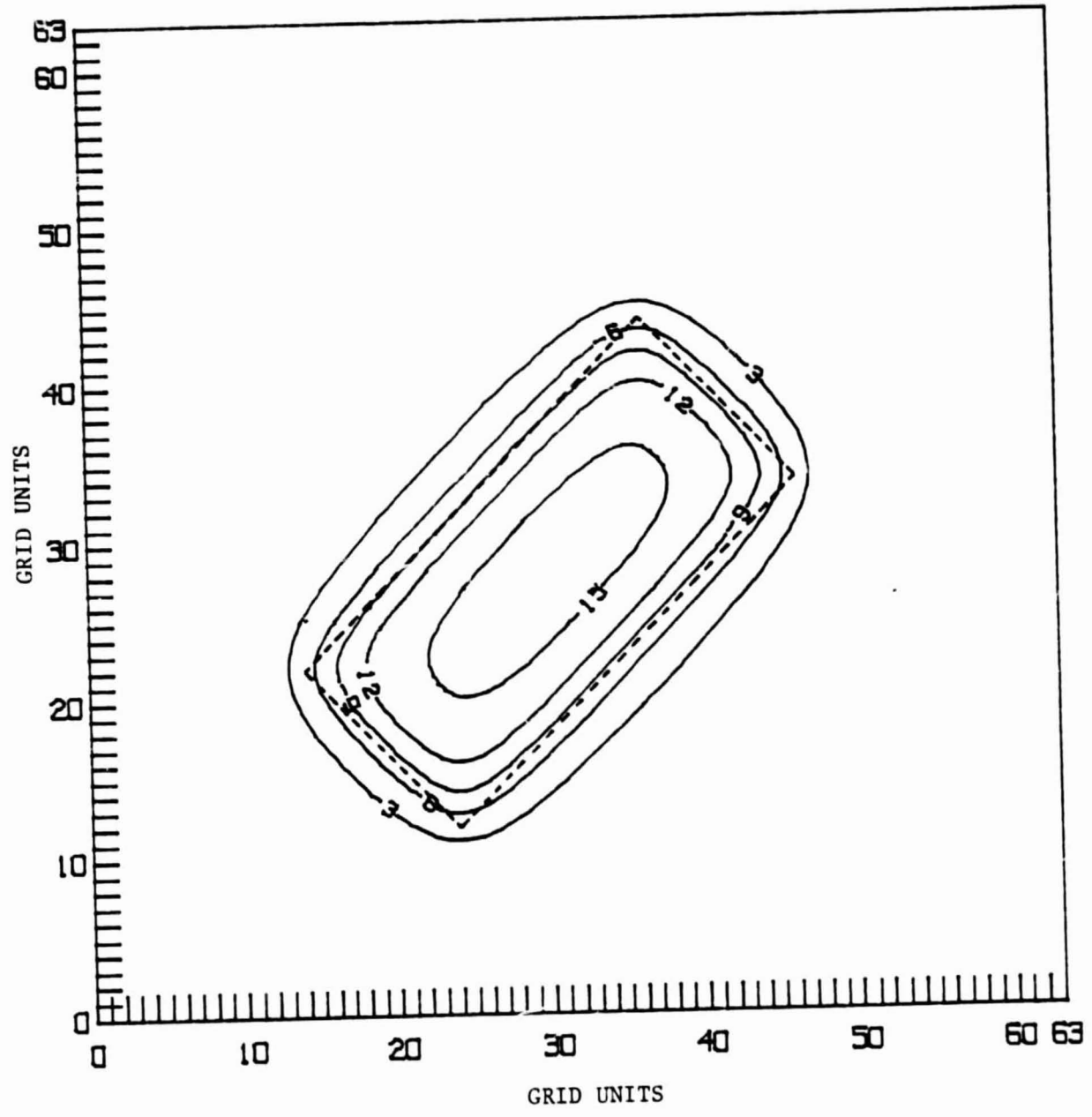Figure 7. The gravity anomaly for a three-dimensional rectangular
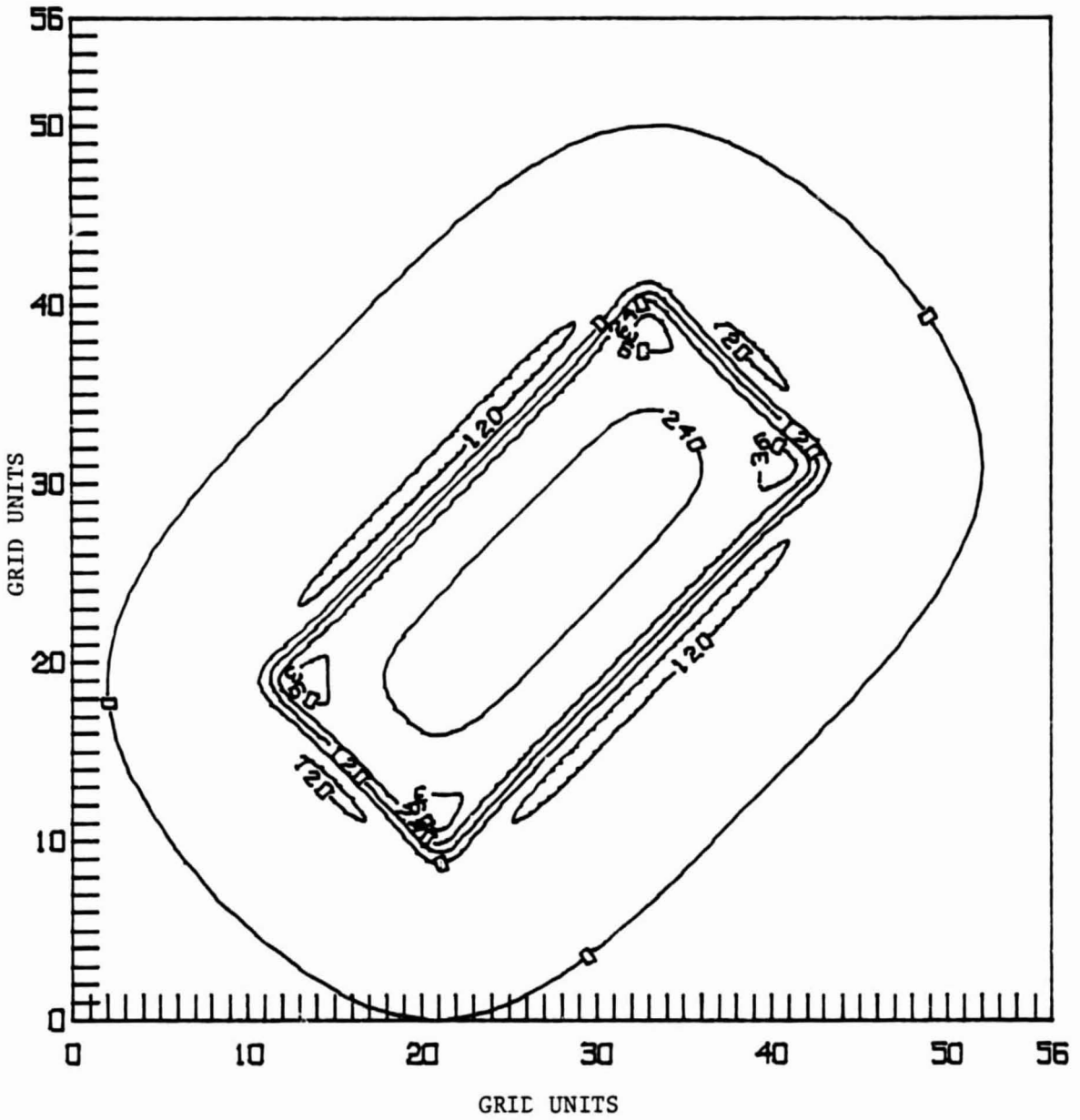prism (contour intervals = 3 mgal)

Figure 8. The third vertical derivative of the gravity field for a three-dimensional rectangular prism (contour interval=120 mgal/di^3)
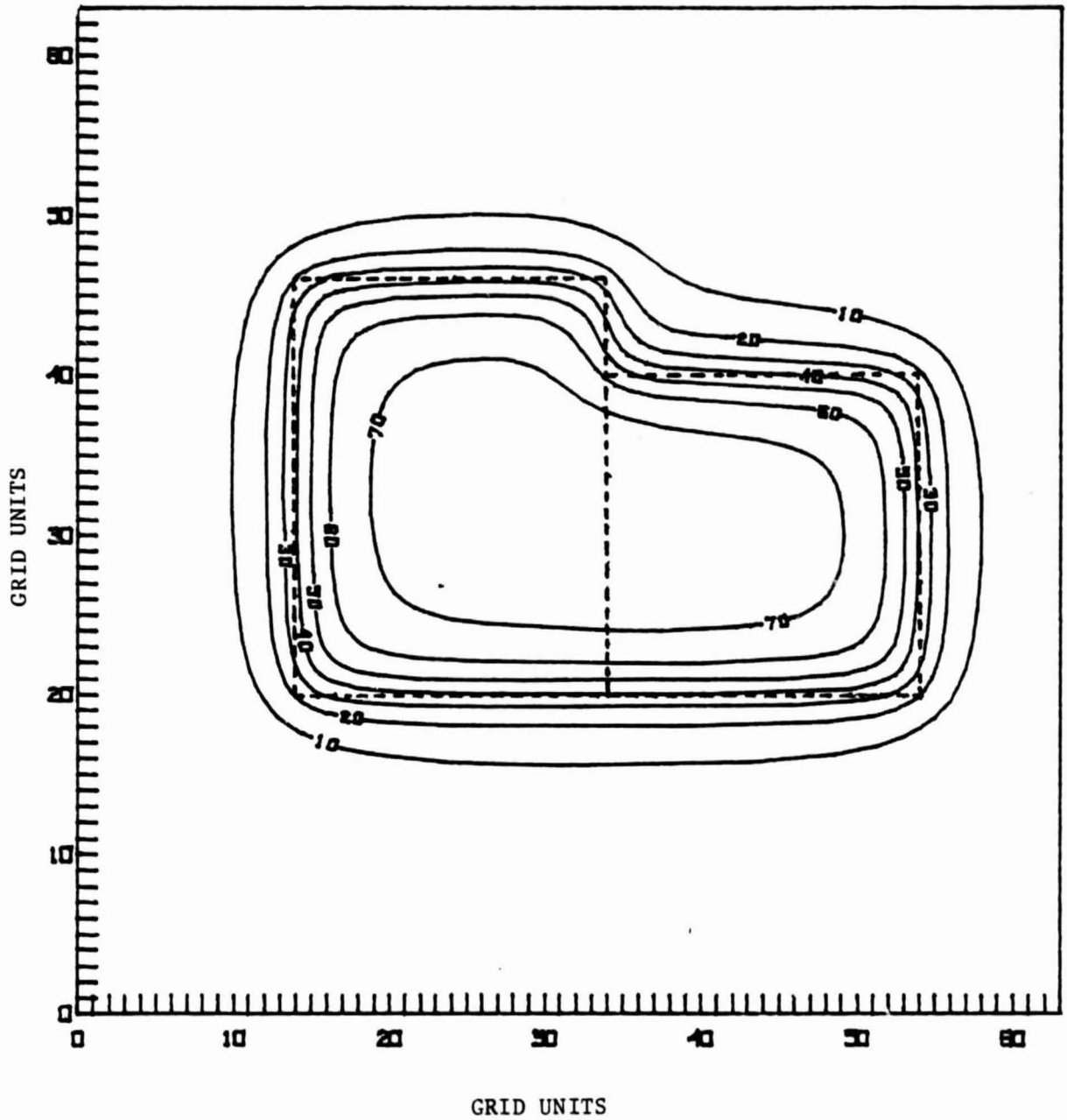
Figure 9. The superimposed gravity anomaly for two three-dimensional
rectangular prisms in contact (contour interval = 10 mgal).

both have a depth of 3.0 and their density contrast is 0.2 gm/cm^3. The map of their superimposed anomaly (Figure 9) gives the impression of being due to a single source with no apparent indication of the inner boundary. On the other hand, the map of the third vertical derivative of the field (Figure 10) reveals the existence of two sources. The zero contour closely follows the outer boundaries with reasonable accuracy, and the contact region is delineated by a well defined low trend. The absence of the zero contour along the contact is caused by the interference of the extrema from each model. This is a persistent problem also in magnetics for cases in which the distance between the bodies is approximately equal to or less than the depth of burial (Jain, 1974).

To simulate an area with several sources, a model with rectangular prisms of various orientations and sizes was evaluated. All the bodies have thicknesses of 1.0. Their upper surfaces are located at a depth of 1.5. Figure 11 gives the superimposed anomaly of the different sources. The relative positions of the bodies are indicated by the dashed lines. The existence of the bodies is easily inferred from the map of the anomaly. However, the exact locations of their boundaries are not quite apparent from the map. On the other hand, in the map of the third vertical derivative (evaluated in the wavenumber domain), the sources are marked more accurately with the zero
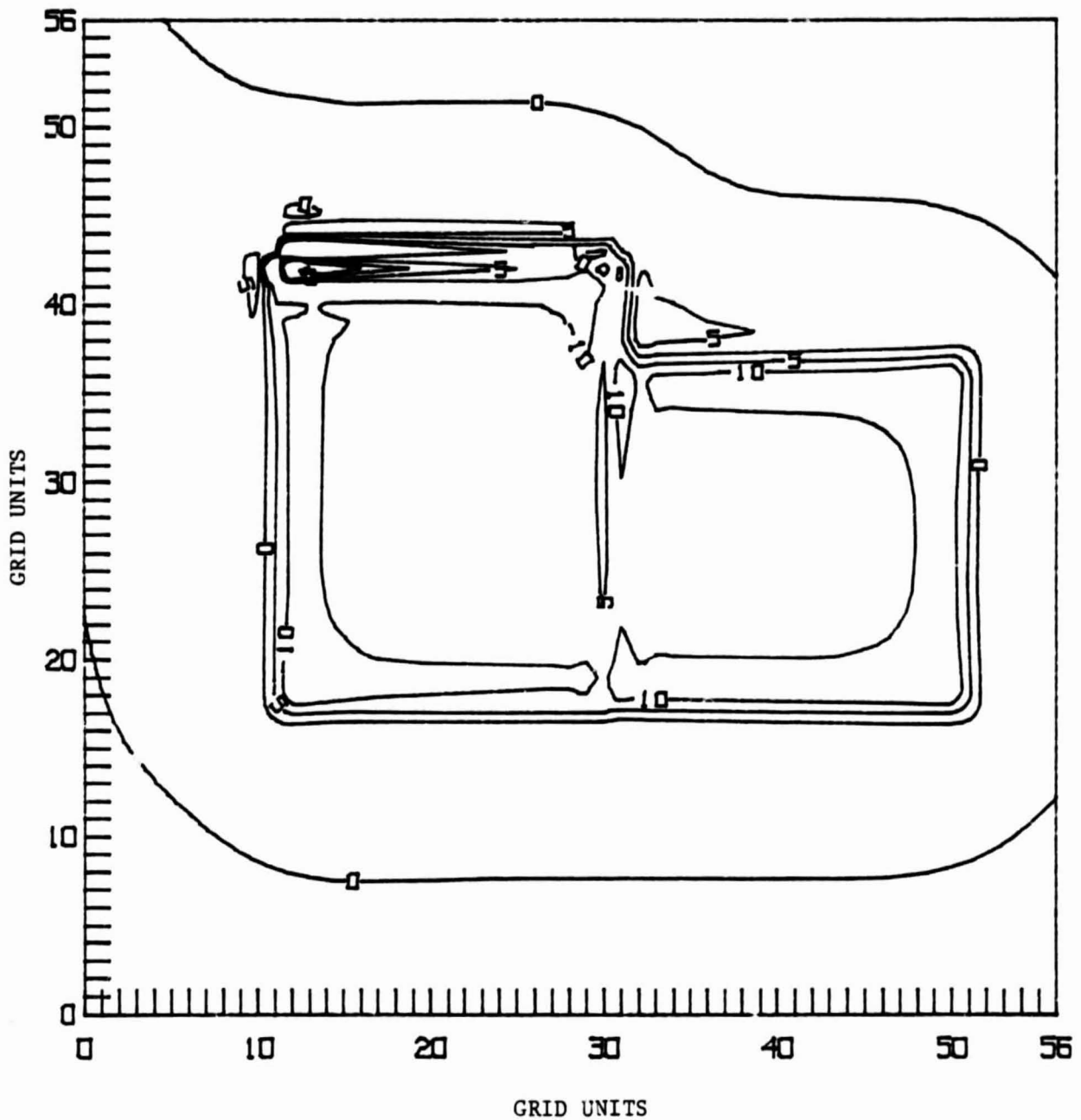
Figure 10. The third vertical derivative of the superimposed anomaly for two rectangular prisms in contact (contcur interval = 10 mgal/di³).

Figure 11. The superimposed gravity anomaly for five prismatic sources with different sizes and orientations (contour interval = 5 mgal).
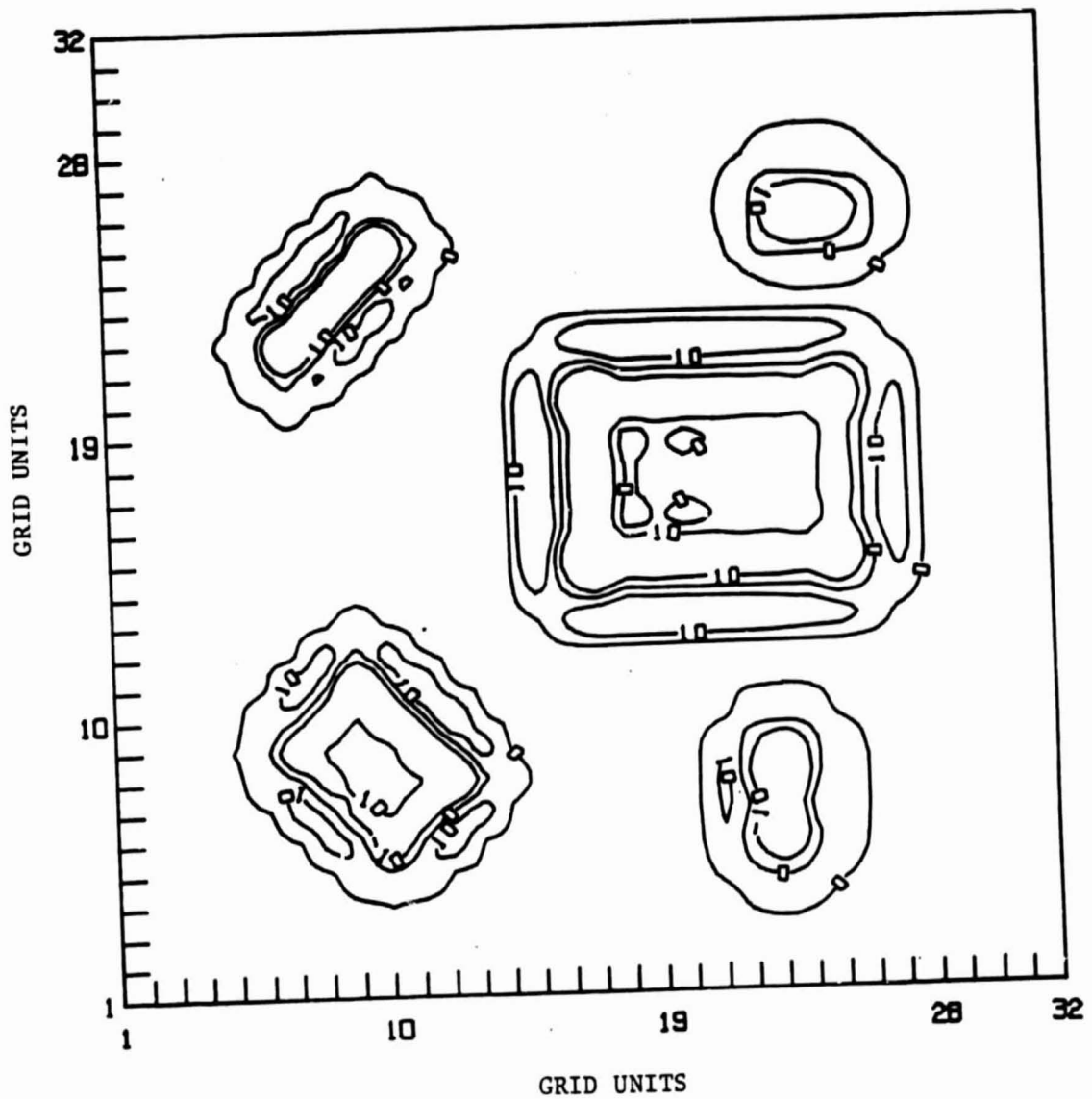
Figure 12. The third · ical derivative of the superimposed anomaly for five prismatic sources with different sizes and orientations. (contour interval=10 mgal/di³)

contour(Figure 12).   It is also noted that the orientation
and relative positions of the various sources are well
preserved by the interpretational technique.

Determination of Depth to the Source

It has been shown in Chapter II that the third vertical
derivative may be employed to obtain the depth of a
prismatic source.   Equation 1 is, in fact, in a form which
would allow one to estimate the depth to the top of an
isolated source.   However, it has also been noted that,
unlike in magnetics, the continuous distribution of density
with depth requires the vertical extent be restricted to
finite values. Thus, the implications of this on the value
of the factor, C (Equation 1),   has been studied in detail
for two-dimensional prismatic models.

The general procedure followed in this study involved
measuring the horizontal distance between the maxima and
minima of the third vertical derivative of a gravity field
(see Figure 3) and then studying its relationship with the
depth to the top of the source.   This was systematically
carried out by employing numerous models with various
widths, thicknesses and depths.

A sample of the depth estimations for two-dimensional
models is given in Table 4.   The thickness varies from 0.2
to 12.0, while the depth and width are kept constant at 2.0
and 12.0, respectively.   For very thick sources (greater

TABLE 4

EFFECT OF THICKNESS ON DEPTH ESTIMATION

Thickness (sampling unit)	Distance between maxima and minima (sampling unit)
0.2	1.8
0.4	1.8
0.6	2.0
0.8	2.0
1.0	2.0
1.2	2.0
1.6	2.0
2.0	2.0
4.0	2.4
8.0	2.5
12.0	2.5

than 8.0) the factor C in Equation 1 is 0.80. For bodies with intermediate thickness (0.6 to 2.0) it is 1.00. As the thickness decreases (below 0.6), C increases to 1.14. The general trend in the value of C is to be expected, since for decreasing thicknesses, the density distribution slowly approaches a distribution equivalent to magnetic monopoles at the top surface of a bottomless prismatic model (Chapter II). For practical purposes, a value of C equal to 1.07 will, in general, give depth estimates with error bounds of less than 7% provided the source is not thicker than two sampling intervals. Similar results are obtained when the above procedure was repeated for various values of the width. Some of the results are shown in Table 5.

TABLE 5

EFFECT OF WIDTH ON DEPTH ESTIMATION

Width (sampl ng unit)	Distance between maxima and minima (sampling unit)
4.0	2.0
6.0	1.8
12.0	1.8
18.0	2.0
24.0	2.0

TABLE 6

DEPTH ESTIMATIONS FOR A FIXED SAMPLING INTERVAL

depth (sampling unit)	Distance between maxima and minima (sampling unit)
0.0	0.4*
1.0	1.2
2.0	2.0
3.0	3.0
4.0	4.0
5.0	5.1
6.0	6.3

*curve very oscillatory

The range of depths the interpretational technique will resolve for a pre-set sampling interval was examined. Table 6 gives selected results for two-dimensional models over a range of depths extending from 0.0 to 6.0. The thickness and width are kept fixed at 1.0 and 12.0, respectively. If

the value of C assumed earlier (1.07) is used, the depth estimates for models located between depths of 2.0 and 5.0 are accurate to within about 9%. However, very shallow sources (less than 1.0) suffer from large errors primarily indicating that the selected grid interval was too large for such shallow depths.

The results given in Tables 4, 5, and 6 cover a wide range of physical parameters that are of practical interest. If, for example, in a field survey the sampling interval is set to 10 km then the models cover depths extending from 0 km to 60 km. The widths considered extend from 40 km to 240 km. For most cases, the percentage error is less than 9%.

It is important to realize that the above results were carried out for isolated sources. In cases where continuous sources (see Figure 12) are encountered, the interference of the maxima and minima of the various sources is to be expected. If it is impossible to select a representative isolated anomaly in such a region of interest, avoiding extrema on the side closer to the boundary of a major source would improve the reliability of the results. Moreover, as has been mentioned earlier, it is imperative to remove the undesirable effects of small, shallow sources prior to applying the operator.

CHAPTER IV

ANALYSIS OF 1° BY 1° MEAN FREE-AIR GRAVITY DATA

In recent years, the theory of global tectonics has greatly improved our understanding of the dynamic processes at lithospheric plate boundaries which are believed to be formed by zones of accretion, subduction, and faulting. These zones, in turn, correspond to rift systems, trenches and transform and/or transcurrent fault zones, respectively (Wilcox, 1974). Linear zones of intense seismic activity and magnetic anomalies have, in the past, been used to identify and delineate such boundaries (Isaacs and Oliver, 1968; Pitman, 1968). More recently, Wilcox (1974) and Kaula (1969, 1971) have utilized global free-air gravity maps for the same purpose.

By comparison, little is yet known about the current tectonic regimes within the interior of continental plates. Earthquake seismology has not been fully utilized for detailed studies of parameters such as focal depth, state of stress, stress drop, and fault plane solutions, partly because only a small percentage of the world's total earthquakes contribute to the intraplate seismic activities (Sykes, 1978). Moreover, the seismograph station coverage, in most areas, is not adequate for detailed studies. This was especially true in the eastern and central United States, where earthquake stations were separated by a

typical distance of about 300 km until recently (Sykes, 1978). Hence, the examination of historical records and present-day seismic activities in this region has, for example, lead to the emphasis of certain trends of seismicity over others (Sbar and Sykes, 1973; Bollinger, 1973, 1975, Woollard, 1958; Richter, 1959; King, 1970).

Thus, at present, there is the need to supplement the investigations of seismic patterns with the study of lineaments revealed by satellite imagery, magnetic and gravity data, and various types of geologic information. In this chapter we will attempt to show how the third vertical derivative of the 1° by 1° mean free-air gravity data may be utilized to enhance certain linear features that may have a bearing on the identification of ancient intraplate boundaries, fault zones, suture zones, continental rift arms, or other major tectonic features.

Global and regional mean free-air maps have over the years provided significant assistance in the examination of tectonic processes both at lithospheric boundaries and in their interiors. One of the major assumptions in such studies has been that sufficiently large areas are in isostatic equilibrium resulting in the mean free-air gravity value being approximately equal to zero (McGinnis, et al., 1979). Locally, however, it may be different from zero. This was inferred from the analysis of gravity data, and from various quantitative and qualitative analyses of

lithospheric bending under pressure (Gunn, 1949; Heiskanen and Meinesz, 1958; McGinnis, 1970). It has been shown that the earth's crust behaves like an elastic plate under a topographic "load" and requires a relaxation distance of about 125 km to 200 km, depending on the geophysical parameters assumed (McGinnis, et at. 1979).

Kaula (1969, 1972) described the tectonic classification of the global gravitational field on the basis of the magnitude and extent of mean free-air gravity anomalies for 5° by 5° areas primarily derived from satellite data. He identified nineteen areas on the earth mostly over trenches, island arcs and active oceanic rises, as mainly positive, and fourteen areas primarily over oceanic and continental basins, as markedly negative. He also determined that the mean free-air gravity anomaly over the eastern United States is zero. Wilcox (1974) in a similar study utilized 1° by 1° mean free-air gravity values to identify patterns that are indicative of plate boundaries. He showed that a narrow belt of intensely negative values usually follows the present-day subduction zones (or trenches), while a belt of intensely positive values usually follows ocean rises and rift systems.

Specifically, within the continental interior of the United States several attempts have been made to study the implications of regional free-air gravity anomaly (Woollard, 1976; McGinnis, 1970). A transcontinental gravity anomaly

profile extending from New York to Los Angeles showed that the United States is in isostatic equilibrium (Woollard, 1958). Similar results were also reported by Heiskanen and Meinesz (1958). In fact, further studies by Woollard (1962) and McGinnis (1970) have shown that the relaxation distance for the continental interior is about 250 km, and the average free-air anomaly value over such large areas would be expected to be approximately equal to zero. Hence, the deviation of the mean values from zero indicates isostatic imbalance. The resulting lineations on the anomaly map may then be utilized to delineate intraplate boundaries or to outline major crustal blocks.

In the next sections, some major lineaments seen in the most recent 1° by 1° mean free-air gravity data of eastern and central United States will be presented. The interpretational procedure will be enhanced by applying the vertical derivative filter developed in the previous chapters. Such linear features, apart from their tectonic significance are also increasingly being recognized as possible indicators of mineral deposits and sites of hydrocarbon accumulations (Saunders, et al., 1976).

Correlations of the Mean Free-Air Gravity Data

with Structure

The gravity field data used in this paper are part of the most recent 1° by 1° mean free-air gravity anomalies of the earth compiled by Rapp (1978). The terresterial gravity values for the eastern and central United States are the updated and expanded versions of the 1978 data set of the Defense Mapping Agency Aerospace Center (DMAAC) and the Lamont-Doherty Geological Observatory. Over some of the continental margins and the ocean areas the data are obtained from GEOS-3 satellite altimetry. The average global accuracy of Rapp's (1978) data set is ±15mgal; however, he noted that in the eastern and southeastern United States, where gravity data are dense, the accuracy is expected to be much better (Rapp, 1978).

To facilitate computer plotting and contouring, the data were interpolated onto a square grid of about 1/4° by 1/4° using a program based on the cubic-spline algorithm published by Davis (1972). The output was then automatically contoured at a 10 mgal interval using the Alber's equal area projection to produce the free-air anomaly map (Figure 13).

The overall pattern of the 1° by 1° free-air anomalies seems to follow the major tectonic provinces, especially in the Appalachian foldbelt. The map is very similar to the 1° by 1° mean free-air map of Woollard (1976) and to the map
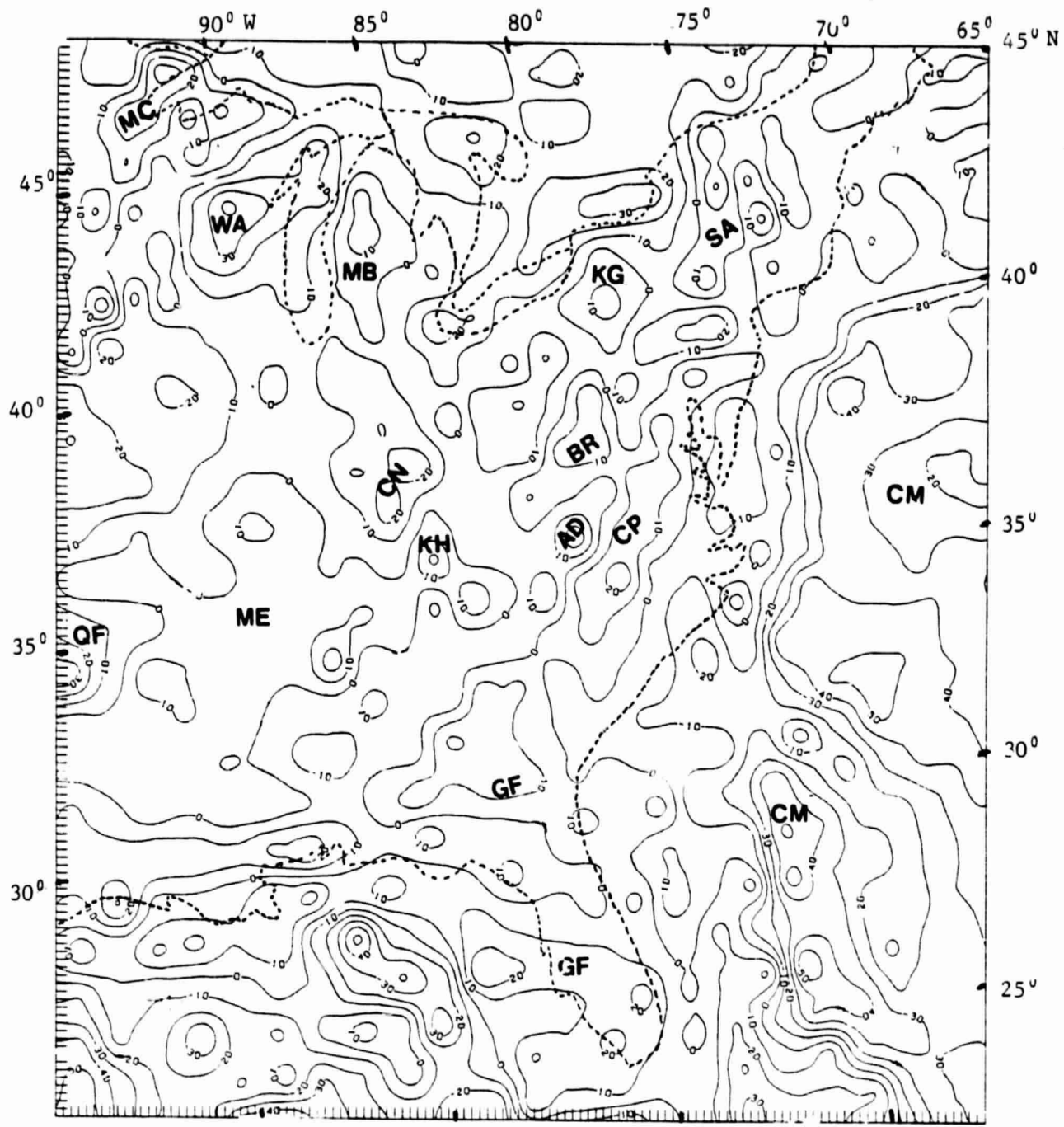
Scale 1:15,000,000

Figure 13. 1° by 1° free-air gravity data for the central and eastern United States. See the text for the meaning of the symbols (contour interval=10 mgal).

constructed by McGinnis, et al., (1979) for values averaged over twelve quadrangles (1° by 0.8°). The anomaly values range from over +30 mgal in the foldbelt to below -50 mgal over the continental margins.

For ease of discussion, the prominent highs and lows that occur over major tectonic regions (Figure 14) are marked with letters on Figure 13. In the eastern central region linear belts of negative and positive anomalies trend in the northeastern direction. The inner Piedmont (AD) and the deepest parts of the Appalachians are associated with a mildly negative anomaly. On the other hand, a strongly positive gravity high follows the east central Piedmont across North Carolina and Virginia (CP). Another prominent high over the Blue Ridge Mountains (BR) is found to the west on line with the Kane gravity high (KG), in Pennsylvania, to the north. The southeastern extension of the large gravity high passes through Georgia (GF) and loops around Florida and heads westward along the Gulf Coast. To the north, a small remnant of the Scranton gravity high joins the positive gravity anomaly associated with the Adirondack Uplift (SA) resulting in a change of the general trend to the north. Over the coastal areas and continental margins to the east, the anomalies are predominantly negative (CM).

The belt of large, positive gravity anomalies in the northwestern corner of Figure 13, is a segment of the so-called midcontinent gravity high (MC), which is even more

Figure 14. Location of major tectonic features in the
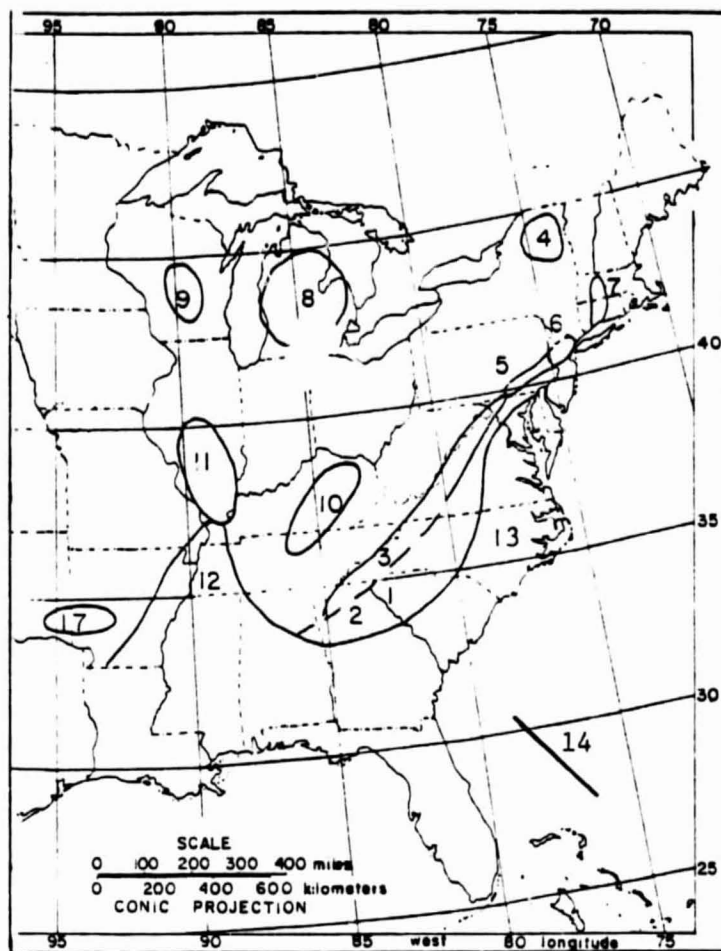central and eastern United States. 1. Piedmont; 2. Brevard
Fault Zone; 3. Blue Ridge;4. Adirondack Uplift;5. Gettysburg
Basin;6. Newark Basin;7. Connecticut Basin;8. Michigan Basin;
9. Wisconsin Arch;10.Cincinati Arch;11. Illinois Basin;12.
Mississippi Embayment;13. Atlantic Coastal Plain;14. Blake
Fracture Zone;17. Ouachita Mountains. Modified after
McGinnis, et al. (1979).

prominently seen in the Bouguer anomaly map of the United States (Woollard, 1964). It is flanked by a negative anomaly over the Wisconsin Arch (WA) and by a positive anomaly over the Michigan Basin (MB). The Mississippi Embayment (ME), to the south, is associated with a broad, mildly positive anomaly that joins the Kentucky gravity high (KH) to the east. There is a gravity low over the Ouachita foldbelts to the west (QF). A negative anomaly corresponds to the Cincinnati Arch (CN).

In general, the association of regional changes of 1° by 1° free-air anomaly with major tectonic regimes seems apparent. As has been noted by King (1970) and Woollard (1976), these anomalies should largely reflect the property of the underlying masses, since the surface relief in the central and eastern United States is, on the average, moderate. There are some notable exceptions to this over areas with high elevation, such as the small gravity high to the southeast of the Kentucky gravity high. One also notes that positive anomalies occur over diverse features such as the Michigan Basin and the Adirondack Uplift, while negative anomalies are observed over the Wisconsin Arch and the Cincinnati Arch. This probably indicates that the anomalies are not caused by shallow sources.

There have been some attempts in the past to understand the nature of the sources that contribute to regional gravity anomalies derived from ground measurements or from

the use of satellite orbital data. Woollard and Khan (1970) conducted a conventional half-width analysis on 12° by 12° free-air gravity data from satellite measurements, and showed that for the major anomalies considered, the centers of the contributing masses have maximum depths that are less than 1000 kms in all cases, and not more than 150 kms in most cases. Woollard (1976) has also made a comparative study of 1° by 1° free-air gravity anomaly with the change of geophysical parameters along the 45°N parallel across the United States. He showed that the pattern of changes of the anomaly are related to the integrated effect of the mean crustal velocity, the values of the crustal thickness, and the upper mantle velocity. In regions where these parameters are high, there are positive gravity anomalies. On the other hand, where they are low, negative anomalies are observed. Hence, it may be concluded that the 1° by 1° free-air anomalies mainly manifest the overall long wavelength changes in crust and upper mantle structure.

Correlation of Data with Regional Lineaments

It has been shown earlier that the zero contour of the third vertical derivative closely outlines the boundaries of an isolated prismatic source. For a continuous distribution of models, the areas of contact were shown to be delineated by well-defined low or high trends. It has also been noted that some anomalies in the mean free-air gravity map (Figure 13) are associated with major tectonic regimes(Figure 14). In fact, one also observes that some linear features in the anomaly map are defined by the zero contour together with some major trends of highs or lows. In this section, the vertical derivative operator will be employed to enhance such linear features in the 1° by 1° mean free-air gravity data for the central and eastern United States.

Sampling theory implies that the scale of features for 1° by 1° (or about 110 km by 110 km) data is roughly 220 km. However, the gravity anomaly map (Figure 13) and its amplitude spectrum (Figure 15) indicate the presence of some higher wavenumber features which might lead to instability problems when obtaining the third vertical derivative. Such problems find their cause in the tendency of the vertical derivative operator to amplify the high wavenumber content of the field spectrum, which is caused by small, shallow sources or by random errors introduced during the data acquisition, digitization, and/or interpolation processes. A detailed inspection of the amplitude spectrum showed that
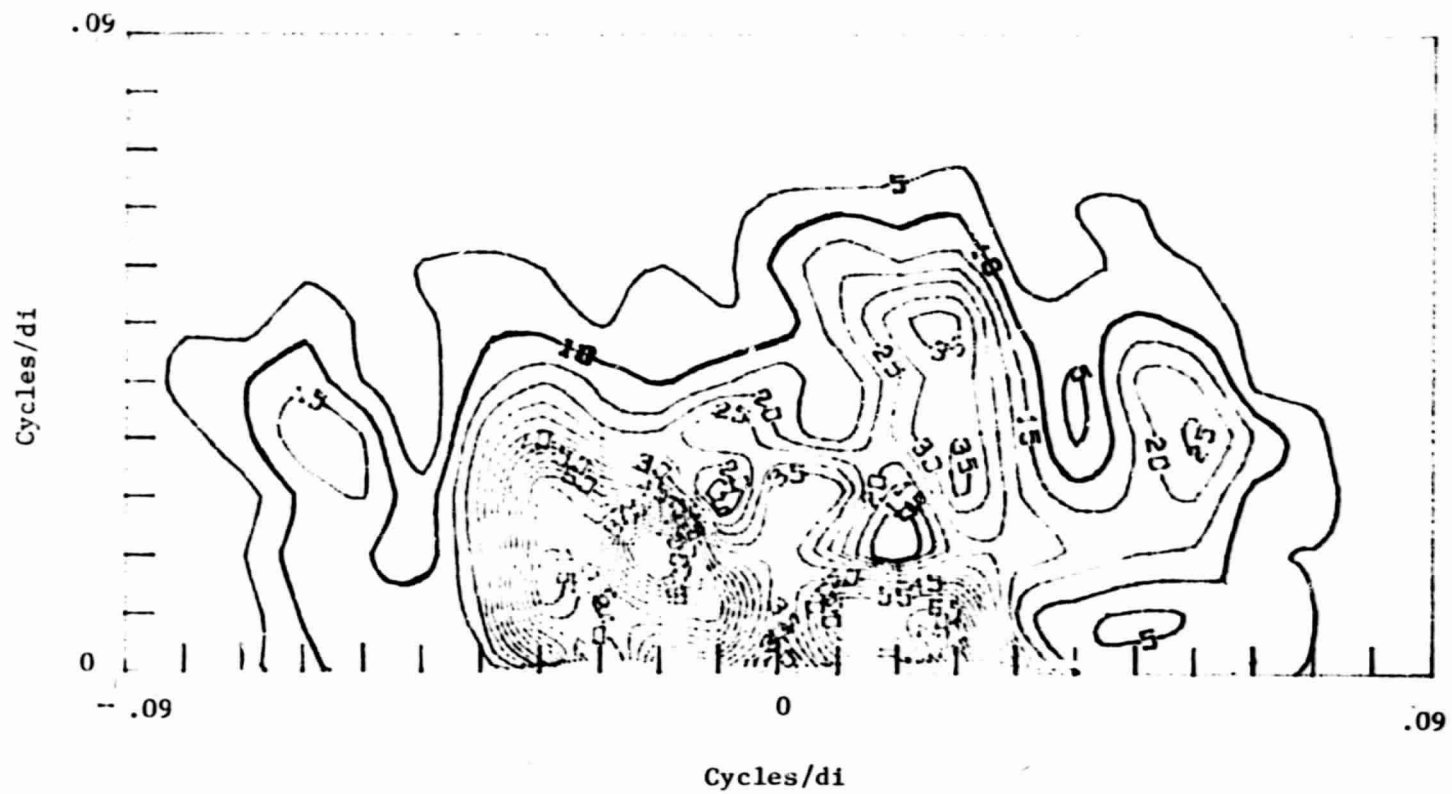
Figure 15. The amplitude spectrum of the gravity data for the central and eastern United States (contour interval = 5 units).

removing wavelengths shorter than about 250 km (or .04 cycles/di) was adequate for our signal processing schemes. The data were convolved with a set of 13 by 13 low-pass filter coefficients that were obtained using an algorithm given by Lavin and Devane (1970). The normalized amplitude response for the filter (Figure 16) shows that it is circularly symmetric for wavenumbers less than about 0.1 cycles/di. Hence, it should not introduce any directional effects in the output.

The filtered version of the free-air data was convolved with the 7 by 7 set of coefficients of the third vertical derivative operator that was developed in the previous chapter (Figure 17). We recall that the operator gives the maxima and minima of the anomaly-curvatures near the boundaries of the isolated body. The distance between the extrema was related to the depth of the top surface of the source, while the zero-contour was found to delineate the outlines of the body. However, in view of the fact that the observed gravity field of the eastern and central United States is the result of the superposition of highly complex mass distributions, the position of the maxima and minima from each source cannot in most instances be accurately isolated. In fact, the interference between the extrema will have the tendency to complicate the already complex picture, as is well illustrated in Figure 17. Hence, the attempt to interpret the results will be directed only
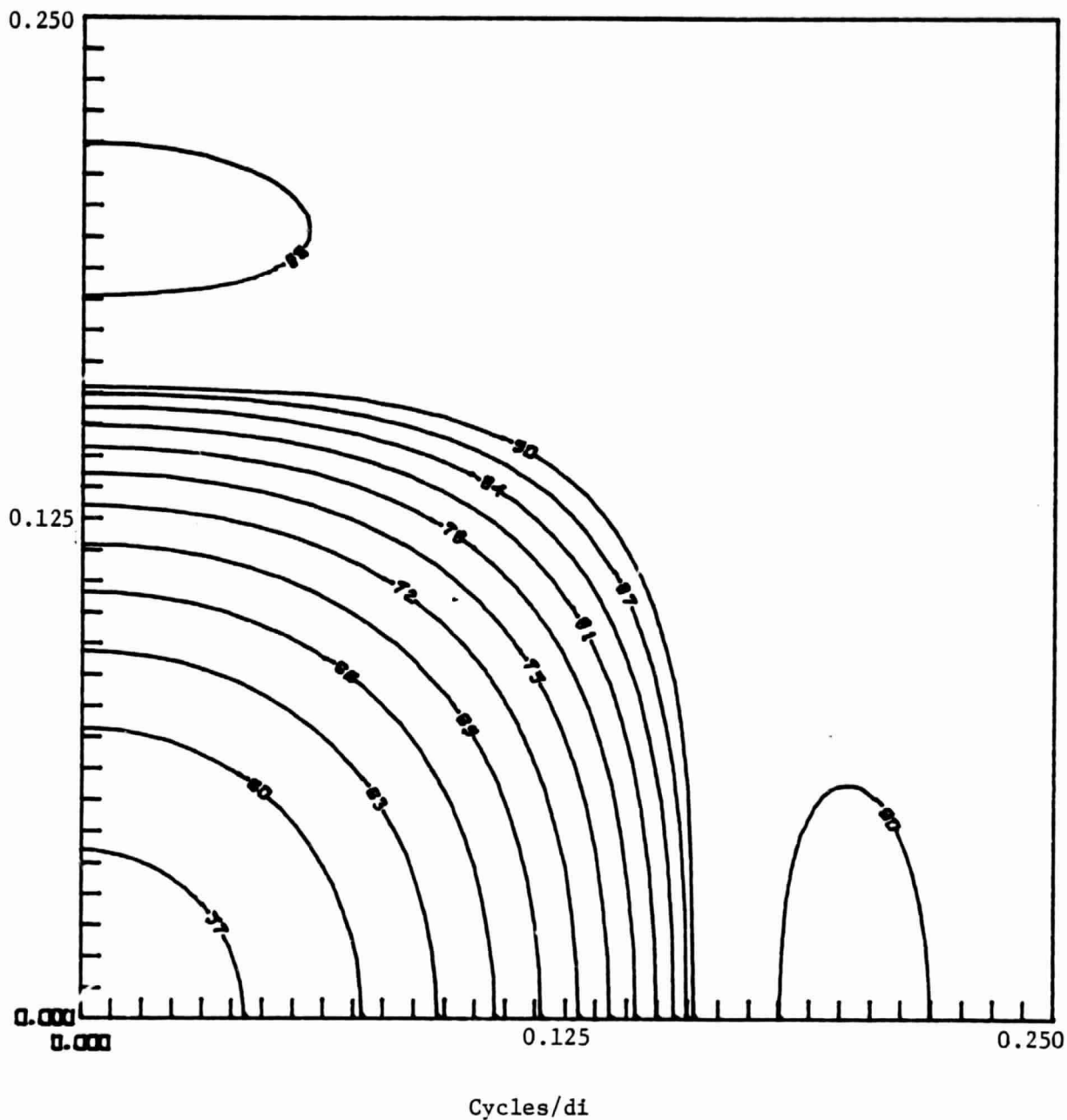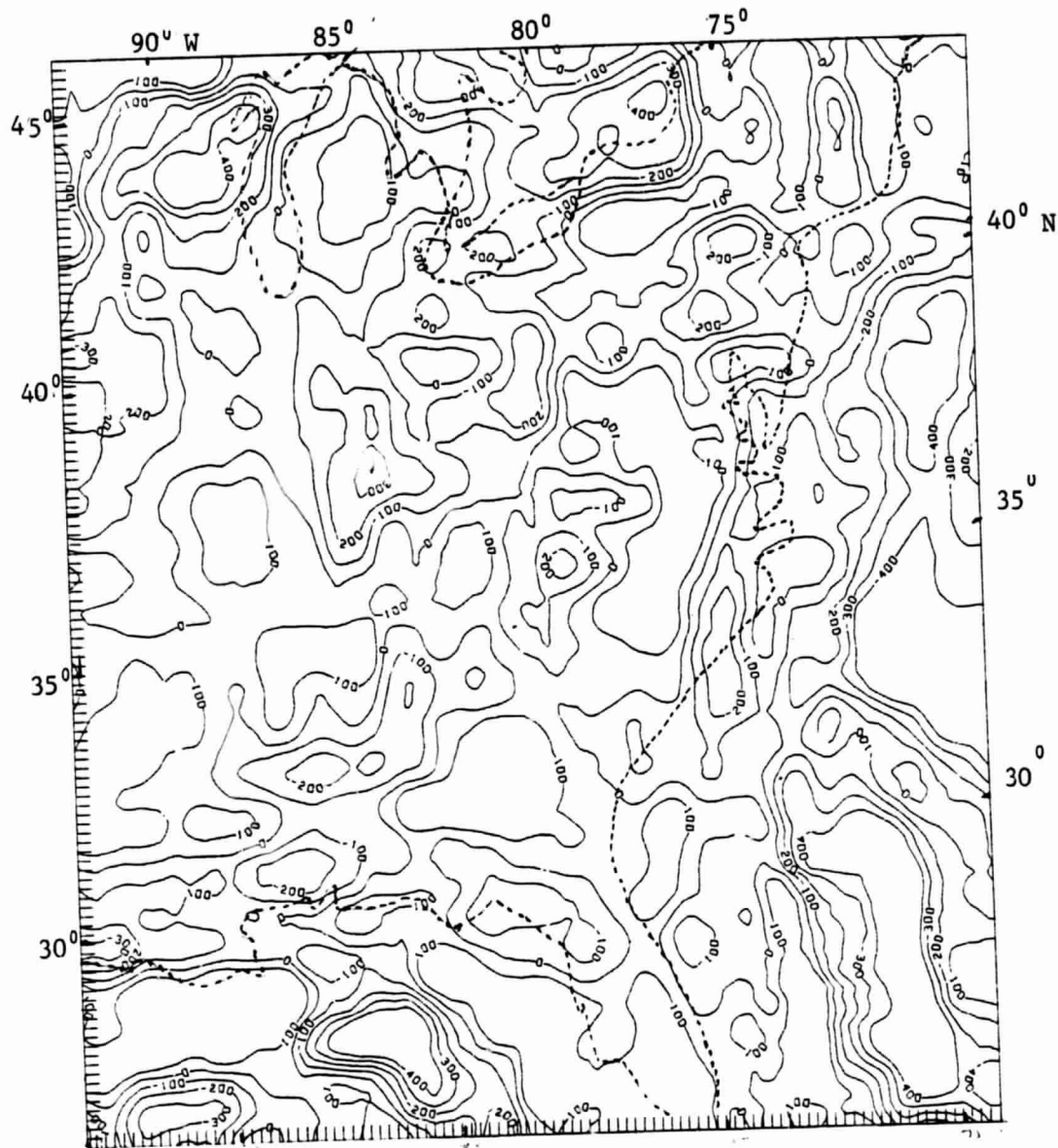
Figure 16. The normalized amplitude response for the low-pass
filter   (contour interval = 3db).

Scale 1:15,000,000

Figure 17. The third vertical derivative of the gravity data for the central and eastern United States.(contour interval= 100 mgal/di^3)

towards the utilization of the zero-contour of the third vertical derivative of the data to identify linear features in the area. These lineaments may then outline the position and areal extent of major crustal blocks. In order to facilitate this interpretation the extrema of the vertical derivative of the data were removed through low-pass filtering, and the resulting map is shown in Figure 18.

It is noted that the maps shown in Figures 13, 17, and 18 have become progressively smaller, though the scale is kept constant. This behavior is caused by the loss of data around the edges during the convolution process.

It should be emphasized that the filtering procedure used does not necessarily eliminate the effect of shallow features, since any particular range of wavenumbers of the spectrum contains the contributions from various sources at different depths. This implies that the gravity effect of regional structures in the sedimentary layer is superimposed on the effects of deeper structures. Likewise, the nature of the 1° by 1° free-air gravity data poses some problems. Even though the data set is the most accurate to date, there are still some problems in the data acquisition and averaging processes that are being worked out (Rapp, 1978).

For this reasons, the analysis, in this section, will be solely aimed at demonstrating the advantages and limitations of the third vertical derivative operator for such a data set. The overall results should, thus, be taken as preliminary in nature.
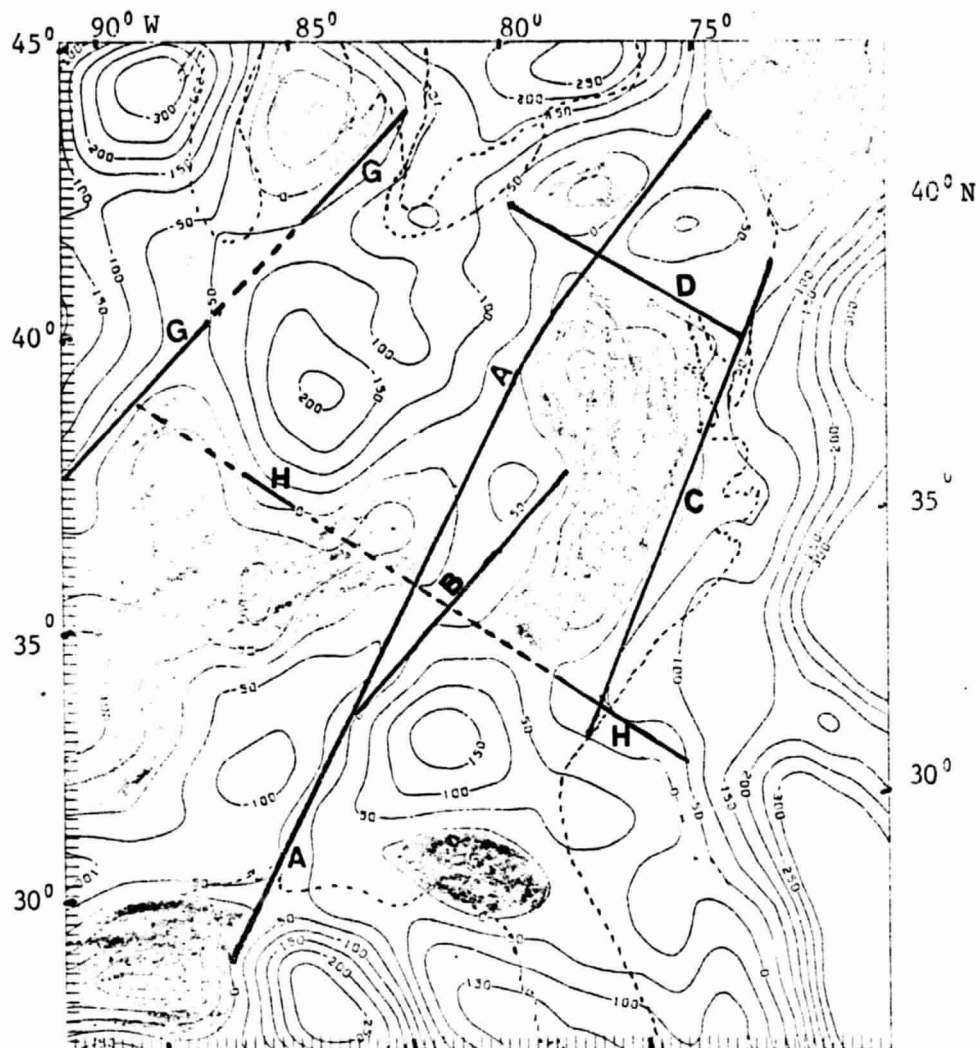
Scale 1:15,000,000

Figure 18. The smoothed version of the third vertical
derivative of the gravity data for the central and eastern
United States (contour interval = 50 mgal/di^3). See the
text for the meaning of the symbols.

Prominent linear features that are enhanced by the vertical derivative filter are shown by solid lines in Figure 18. These lineaments are inferred from zones delineated by the zero contour, and from areas along which high or low trends are aligned or terminated. Only the very distinct features that appear to have possible bearing on identifying major crustal blocks are marked. The overall picture in Figure 18 seems to show a bias toward the dominance of major lineaments in the northeast-southwest directions. Affleck (1963, 1970) reported that the aeromagnetic data showed a similar trend as well as a few others. (He also reported that the vertical derivative filter was employed to enhance the interpretation of the data).

In order to form some framework for the analysis we have assigned a letter to each of the linear features (Figure 18). Lineament A, which is, perhaps, the most persistent one, correlates with the so-called New York-Alabama magnetic lineament (King and Zeitz, 1978) all the way from the southern part of New York to eastern Tennessee. It swings to the southeast in Alabama, where the "magnetic" lineament was absent and was actually augmented using the Bouguer gravity anomaly (King and Zeitz, 1978). We also note that lineament A tends to follow the west side of the Appalachian gravity low (AD in Figure 13) and also separates a zone of predominately north trending gravity anomalies to the

northwest from a zone of northeast trending anomalies to the southeast. This is clearly seen in Figure 17. Moreover, as has been noted by Watkins (1964) and King and Zeitz (1978) for the New York-Alabama lineament, A seems to bound an active seismic zone over the eastern part of the Appalachian basin extending from New England to eastern Tennessee (Figure 19). It also parallels the New Madrid earthquake zone to the 'est. King and Zeitz (1978) have suggested that the zone may represent an ancient intraplate boundary between the highly deformed Appalachian foldbelt and the stable craton of the continental interior.

Lineament B traces the Brevard fault zone throughout its mapped length that extends from southern Virginia to the coastal plains of Alabama (Reed and Bryant, 1961; King, 1977). Saunders and Hicks (1976) have noted that satellite imagery suggests further extensions northward into Maine and southward to the Gulf coast. However, lineament B is truncated in Virginia and merges with New York-Alabama lineament to the south.

Along the eastern boundary of the Piedmont ("the fall line"), there is a belt of earthquakes that extends roughly from New Jersey to Alabama, along which many major faults have been recognized (Agarwal and Sykes, 1978; Higgins et al., 1974). A focal mechanism solution for an earthquake around Wilmington, Delaware, showed dip-slip movement on a nearly vertical fault oriented in a northeast direction
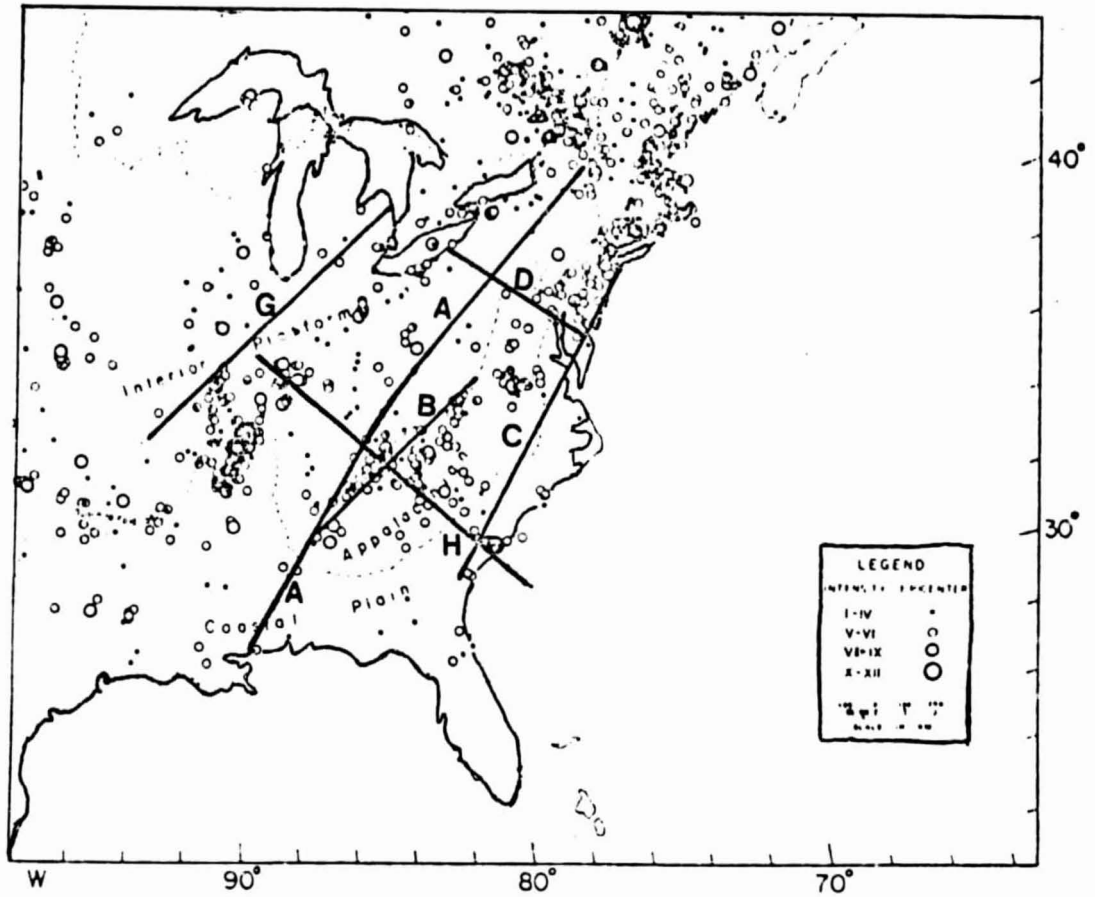
Figure 19. Seismicity map for the central and eastern United States, 1534-1971. Modified after Sykes (1978). See the text for the meaning of the symbols.

(Sbar, et al., 1975). Higgins ,et al. (1974) have also noted that the pattern of aeromagnetic anomalies suggest a system of faults that runs from New York to Virginia. Lineament C appears to correlate with such a zone of faulting and seismic activity. In the north this linear feature intersects lineament D, which traces the axis defined by the Appalachian Salient between South Mountain and the Newport gravity and magnetic high. Further extension of lineament D to the northwest follows the Tyrone-Mt. Union lineament.

In the northwestern part of the region, lineament G appears to bound the New Madrid earthquake zone. This seismic region is the most active in the central and eastern United States. Historic records that include two large earthquakes of 1811 and 1812, and recent activities are concentrated along the northern part of the Mississippi Embayment, which is associated with northeast trending faults, and large magnetic anomalies (Sykes,1978).

Lineament "H," in the south, partly defines the Blake Fracture Zone, an ocean floor topographic feature where a left lateral offset (100km) of magnetic lineaments has been observed (Pitman and Talwani,1972). On land, extensions of this linear feature are inferred from satellite imagery and geophysical data. Bollinger (1972, 1973), in a study of historic earthquakes and recent activities defines a South Carolina-Georgia zone of northwesterly seismic trend which

is not far from an extension of the fracture zone. The
trend is also delineated by several igneous intrusions
(King, 1961; De Boer, 1967), and by some prominent magnetic
anomalies indicative of mafic and ultramafic rocks at depth
(Popenoe and Zeitz, 1977). It is also interesting to note
that the seismic area close to Charleston, South Carolina,
falls close to the intersection of this linear feature with
lineament C.

At this stage of the project, one may attempt to identify
the crustal blocks that are bounded by the major lineaments
keeping in mind the problems brought on by the superposition
of shallow and deep sources. For example, King and Zeitz
(1978) have recognized the aseismic area northeast of the
Mississippi Embayment as a more stable crustal block. It is
bounded by lineament A in the east and the New Madrid
seismic zone in the west. The southern boundary is the zero
contour of the Mississippi Embayment. Its border in the
north is not clear from the map though an extension of
lineament D is a possible candidate. Another crustal block
is, perhaps, what Sykes (1978) calls the Blue Ridge Dome.
This block is roughly bounded by the zero contour (Figure
18) marked by lineaments A, B, C, D, and an approximate
ex nsion of lineament H on the south. It is possible that
one will be tempted to continue such a scheme over the whole
region. For instance, the shaded areas in Figure 18 that
are delineated by the zero contours are some likely

candidates for crustal blocks. One may then attempt to study the seismic, magnetic and other data for the indicated blocks to determine the difference between their average properties. However, as it has been stressed earlier, any detailed and reliable analysis should wait until the influence of the sedimentary layer is identified and eliminated.

CHAPTER V

CONCLUSIONS

The major intent of this study has been to investigate the conditions whereby an interpretational technique that has been extensively used for aeromagnetic data analysis may be extended to gravity field interpretation. The technique was based on the fact that, for an isolated, bottomless rectangular prism, the zero contour of the second vertical derivative of its magnetic field closely outlines its top surface (Vacquier et al., 1958). Moreover, the horizontal distance between the plotted maxima and minima of the derivative gives an estimate of the depth to the source (Jain, et al., 1974). An examination of Poisson's theorem indicated that an extension of the method to gravity field analysis was possible. It implied that the second vertical derivative of the magnetic field is equivalent to the third vertical derivative of the gravity field. However, The continuous distribution of density with depth required that, when using the gravity field, the prismatic model had to be restricted to a finite thickness in order to avoid a singularity. Hence, a detailed model study was carried out to determine the effects of the thickness factor on the interpretational technique.

The rectangular prismatic model with finite thickness was examined extensively because of its wide applications in the

investigation of varied geological structures. The space
domain expression of its gravity effect showed that its
parameters were contained in coupled terms . This made the
analytical evaluations of the third vertical derivative
rather interactable. Hence, for the sake of simplicity,
most of the analysis was carried out in the wavenumber
domain. In some cases, it was necessary to employ a
derivative operator designed in the spatial domain in order
to circumvent severe truncation effects.

An examination of the sensitivity of the interpretational
technique to sampling interval demonstrated that the finer
the grid spacing the more accurate the computed results.
However, a sampling interval of about 0.2 times the width
for the numerical models gave adequate results in outlining
the top surface of the source, while a value of 0.1 was
required for estimating their depth of burial. In cases
where the grid spacing was coarser, interpolation to finer
spacing using the bi-cubic spline interpolation in the
spatial domain and padding with zeroes in the wavenumber
domain were found effective in improving the results.

The model study covered a wide range of physical
parameters that were of practical interest. If, for
instance, a grid interval in a field survey is assumed to be
10 km, the range of thicknesses studied varied from 2 km to
200 km, the depths considered extended from zero to 70 km,
and the width varied from 20 km to 240 km. The overall

results demonstrated that, for thicknesses ranging from 0.2 to 20.0 sampling intervals, error bounds of less than 8 percent are to be expected on outlining the edges of the source. On the other hand, error bounds for the depth estimate would be less than 9 percent if the thickness is smaller than twice the grid interval.

The versatility of the interpretational technique was illustrated by evaluating the superimposed anomalies of several three-dimensional rectangular prisms. It was demonstrated that the zero contour of the third vertical derivative of the gravity field closely outlines the top surface for isolated sources. In cases where the models were in contact, the boundaries were delineated by well defined low or high trends. The orientations and relative locations of the various models were also well preserved by the technique. However, the depth estimation for sources in contact was made difficult by the interference of their extrema. In such cases, using extrema that are away from the contact region gave better results.

Finally, an attempt was made to analyze the most recent $1°$ by $1°$ free-air gravity data for the central and eastern United States. The anomaly map produced was found to be very similar to that of Woollard(1976) and McGinnis, et al., (1979). The general pattern of the anomalies appears to follow the major tectonic regimes. It was understood that the major high and lows primarily reflect the effect of the

underlying masses, since the mean surface elevation in the region is moderate. Moreover, the observation of, for instance, large positive anomalies over both basins and uplifts (e.g; the Michigan Basin and Adirondack Uplift) seems to indicate that the sources of the anomalies are not shallow in nature. In fact, the overall picture ,appears to support the suggestion by Woollard (1976) that the free-air gravity anomaly reflects the integrated effect of the mean crustal and upper mantle structure.

The interpretational technique developed in this pa, er was employed to enhance the linear features observed in the 1° by 1° free-air gravity data. Prior to this, the high wavenumber content of the field spectrum was removed through low-pass filtering. However, it is likely that the filtering procedure did not necessarily eliminate the effect of all shallow sources. Hence, only a preliminary analysis of the most distinct lineaments was attempted. In spite of this restriction,the correlation of the inferred linear features with some seismic trends and magnetic lineaments was demonstrated. Some possible crustal blocks were also delineated by the zero contour of the third vertical derivative of the field data.

Further work should be done on the relationship between the inferred crustal blocks and the basement structure in the region. This probably involves isolating and removing the effect of the regional stuctures in the sedimentary

layer.   Further work   should also be done   in comparing the
seismic,   magnetic and   other   geophysical   data   for   the
inferred crustal blocks.

REFERENCES

Affleck,J., Magnetic anomaly trend and spacing patterns, Geophs., 28, 379-395, 1963

Affleck,J., Definitions of regional structures by magnetics, in the Megatectonics of Continents and Oceans, edited by H. Johnson and B.L. Smith, Rutgers University Press, New Brunswick, 74-112, 1970

Agarwal,B.N.P., and T. Lal, A generalized method of computing second derivative of gravity field , Geophys. Pros., 20, 385-394, 1972

Agarwal,B.N.P., and L.R. Sykes, Earthquakes, faults, and nuclear power plants in southern New York-northeastern New Jersey, Science, 200, 425-429, 1977

Battacharyya, B.K., A method for computing the total magnetization vector and the dimensions of a rectangular block-shaped body from magnetic anomalies, Geophys., 31, 74-96, 1966

Battacharyya, B.K., Magnetic anomalies due to prism-shaped bodies with arbitrary polarization, Geophys., 29, 517-531, 1964

Bollinger, G.A., Historical and recent seismic activity in South Carolina, Bull. Seism. Soc. Amer., 62, 851-864, 1972

Bollinger, G.A., Seismicity and crustal uplift in the southereastern United States, Amer. J. Sci., 273-A, 396-408, 1973

Bollinger, G.A., A micro-earthquake survey of the central Virginia seismic zone, Earthquake Notes, 46, 3-13, 1975.

Carrol, R., Spectral analysis of gravity effect due to finite mass distribution, M.S. thesis, Pennsylvania State University, 1973

Cooley, J.W., and J.W. Tuckey, An alogrithm for machine calculation of complex Fourier series, Math. of Comput., 19, 297-301, 1965

Cordell, L., and P.T. Taylor, Investigation of magnetization and density of North American seamount using Poisson's theorem, Geophys., 36, 199-937, 1971

REFERENCES - cont.

Davis, T.M., and A.L. Kontis, Spline interpolation algorithms for track-type survey data with application to the computation of mean gravity anomalies, NAVOCEANO TR-226, 82p., 1970

De Boer, J., Paleomagnetic-tectonic study of Mesozoic dike swarms in the Appalachians, J. Geophys. Res., 72, 2237-2250, 1967

Elkins, T.A., The second derivative method of gravity interpretation, Geophys., 16, 29-50, 1951

Fuller, B.D., Two-dimensional frequency analysis and design of grid operators, Mining Geophysics, vol. II, Society of Exploration Geophysicists, New York, 708p., 1967.

Garland, G.D., Comparisons of gravitational and magnetic anomalies over certain structures in southern Ontario, The Canadian Mining and Metallurgical Transactions, 59, 340-345, 1951b.

Green, R., Remanent magnetization and the interpretation of magnetic anomalies, Geophys. Prosp., 8, 267-278

Gunn, R., Isostasy-extended, J. Geo_., 57, 263-278, 1949.

Henderson, R.G., and I. Zeitz, Analysis of total magnetic intensity anomalies produced by point and line sources, Geophys., 13, 428-436, 1948.

Henderson, R.G., A comprehensive system of automatic computation in magnetic and gravity interpretation, Geopyhs., 25, 569-585, 1960.

Higgins, M.W., I. Zeitz, and G.W. Fisher, Interpretation of aeromagnetic anomalies bearing on the origin of upper Chesapeake Bay and river course changes in the central Atlantic seaboard region: Speculations, Geology, 2, 73-76, 1974

Isaacs, B., and J. Oliver, Seismology and the new global tectonics, J. Geophy.,Res., 73, 1968.

Jain, S., W. Shuur,and C.E. Curtis, Source prarameter map: A new aid to aeromagnetic data interpretation, Aero Service publ., 23p., 1974

REFERENCES - cont.

Kanasewich, E.R., and R.G. Agarawal, Analysis of combined gravity and magnetic field in wavenumber domain, J. Geophys. Res., 75, 5702-5712, 1970.

Kaula, W.M., A tectonic classfication of the main features of the earth's gravitational field, J. Geophys. Res., 4807-4826, 1969.

Kaula, W.M., Global gravity and tectonics, in the Nature of the Solid Earth, edited by E.C. Robertson, McGraw Hill, New York, 385-405, 1972.

King, P.B., Systematic pattern of Triassic dikes in the Appalchian region, U.S. Geol. Surv. Prof. Pap., 424-B, 93-95, 1961

King, P.B., Tectonics and geophysics of eastern United States, in Megatectonics of Continents and Oceans, edited by H. Johnson, and B.L. Smith, Rutgers University Press, New Brunswick, 74-112, 1970.

King, P.B., The evolution of North America, Princeton University Press, Princeton, 197p., 1977.

King, E.R. and I. Zeitz, The New York-Alabama lineament: Geophysical evidence for a major crustal break in the basement beneath the Appalachian basin, Geol., 6 , 312-318, 1978.

Lavin, P.M., and J.F. Devane, Direct design of two-dimensonal wavenumber filters, Geophys., 35, 1073-1078, 1970

Lundback, A., Combined analysis of gravimetric and magnetic anomalies and some paleomagnetic results, Geophys. Pros., 4 , 226-235, 1956

McGinnis, L.D., M.G. Wolf, J.J. Kohsman, and C.P. Ervin, Regional free-air gravity anomalies and tectonic observations in the United States, J. Geophys. Res., 84, 591-601, 1979.

McGinnis, L.D., Tectonics and gravity field in the continental interior, J. Geophs. Res., 75, 317-331, 1970.

REFERENCES - cont.

Nagy, D., The gravitational attraction of a right rectangular prism, Geophys., 31, 362-371, 1966.

Pitman, W.C., E.M. Herron, and J.R. Heirtzler, Magnetic anomalies in the Pacific and sea-floar spreading, J. Geophys. Res., 73, 1968.

Pitman, W.C., and M. Talwani, Sea-floar spreading in the north Atlantic, Geol. Soc. Amer. Bull., 83, 619-646,1972.

Popenoe, P.and I. Zeitz, The nature of the geophysical basement beneath the coastal plain of South Carolina and northern Georgia, U.S. Geol. Surv. Prof. Pap., 1028-I, 119-137, 1977.

Rapp, R.H., A combined terresterial-altimeter 1° by 1° mean gravity anomaly field, A paper presented at the eighth meeting of the International Gravity Commission, Paris, 1978.

Reed, J.C., and B. Bryant, Evidence for strike slip faulting along the Brevard Zone in North Carolina, Bull. Geol. Soc. Amer., 75, 1177-1196, 1964.

Richter, C.F., Seismic regionalizations, Bull. Seism. Soc. Amer., 49, 123-162, 1959.

Robinson, E.S., The use of Poisson's relation for the extraction of psuedototal magnetic field intensity from gravity observations, Geophys., 36, 605-608, 1971.

Ross,H.P., and P.M. Lavin, In-situ determination of remanent magnetic vector of two-dimensional tabular bodies, Geophys., 31, 949-962, 1966.

Saunders, D.E., and D.E. Hicks, Regional geomorphic lineaments on satellite imagery: Their origin and applications, A paper presented at 2nd International conference on basement tectonics, Newark, Del., 13-17 July 1976.

Sbar, M.L., et al., The Delware-New Jersey earthquake of February 28, 1973, Bull. Seis. Soc. Amer., 65, 85-92, 1975.

REFERENCES - cont.

Sbar, M.L., and R.L. Sykes, Contemporary compressive stress and seismicity in eastern North America: An example of intraplate tectonics, Geol. Soc. Amer. Bull., 84, 1861-1882, 1973.

Sykes, L.R., Intraplate seismicity, reactivation of preexisting zones of weakness, alkaline magmatism, and other tectonism postdating continental fragmentation, Rev. Geophys. and Space Phys., 16, 621-688, 1978.

Talwani, M., and J.R. Heirtzler, Computation of magnetic anomalies of arbitrary shape, In Computers in Mineral Indusries, Part I, 9 , 464-480, 1964.

Talwani, M., Computations with the help of a digital computer of magnetic anomalies caused by bodies of arbitrary shape, Geophys., 30 , 797-811, 1965

Vacquier, V., W.C. Steenland, R.G. Henderson, and I. Zeitz, Interpretation of aeromagnetic maps, Geol. Soc. Amer. Mem. 47, 151p., 1958.

Watkins, J.S., Regional geologic implications of the gravity and magnetic fields of a part of eastern and southern Kentucky, U.S. Geol. Surv. Prof. Pap., 516-A, 17p, 1964.

Wilcox, L.E., Mapping plate boundaries with reference to mean gravity anomalies, Defense Mapping Agency and Aerospace Centre Tech. Pap., 74-003, 17p., 1974

Woollard, G.P., Areas of tectonic activity in the United States as indicated by earthquake epicenters, EOS Trans. Amer. Geophs. Union, 39, 1135-1150, 1958

Woollard, G.P., and M.A. Khan, A review of the satellite-determined figures of geoid and their geophysical significance, Pacific Sci., 24, 1-28, 1970.

Woollard, G.P., Regional changes in gravity and their relation to crustal parameters, in Volcanoes and Tectonosphere, edited by H. Aoki and S. Iizuka, Tokai University Press, Shimizu, Japan, 237-258, 1976.

END

DATE

FILMED

N 29 1982